permafrost cci

CCI+ PHASE 1 – NEW ECVS

PERMAFROST

D4.1 PRODUCT VALIDATION AND INTERCOMPARISON REPORT (PVIR)

VERSION 3.0

30 SEPTEMBER 2021

PREPARED BY

b·geos

GAMMA REMOTE SENSING

UiO : University of Oslo

AWI

UNI FR
UNIVERSITÉ DE FRIBOURG
UNIVERSITÄT FREIBURG

Stockholm University

West University of Timisoara

TERRASIGNA

Document Status Sheet

Issue	Date	Details	Authors
1.0	30.09.2019	CRDPv0 evaluation	B. Heim, M. Wieczorek (AWI), A. Bartsch, C. Kroisleitner (B.GEOS) Cécile Pellet, Reynald Delaloye, Chloé Barboux (UNIFR)
2.0	30.09.2020	Update of all evaluation results based on CRDPv1	A. Bartsch (B.GEOS), B. Heim M. Wieczorek (AWI), Cécile Pellet, Reynald Delaloye (UNIFR)
2.1	14.01.2020	Inclusion of temporal stability	M. Wieczorek, B. Heim (AWI)
3.0	30.09.2020	Update of evaluation results based on CRDPv2	B. Heim, S. Lisovski (AWI), Cécile Pellet, Reynald Delaloye (UNIFR), A. Bartsch (B.GEOS)

Author team

Birgit Heim, AWI

Simeon Lisovski, AWI

Mareike Wieczorek, AWI

Cécile Pellet, UNIFR

Reynald Delaloye, UNIFR

Annett Bartsch, B.GEOS

Dan Jakober, B.GEOS

Georg Pointner, B.GEOS

Tazio Strozzi, GAMMA

ESA Technical Officer: Frank Martin Seifert

EUROPEAN SPACE AGENCY CONTRACT REPORT

The work described in this report was done under ESA contract. Responsibility for the contents resides in the authors or organizations that prepared it.

TABLE OF CONTENTS

EXECUTIVE SUMMARY

This document presents the Product Validation and Intercomparison Report (PVIR) version 3, an important deliverable of the European Space Agency (ESA) Climate Change Initiative (CCI) Permafrost project. ESA CCI is a global monitoring program with the major aim to provide long-term Earth Observation (EO)-based Essential Climate Variables (ECVs) products serving the climate modelling and climate user communities. Permafrost has been selected as one of the ECVs which are elaborated during Phase 1 of CCI+ (2018-2021). The required parameters for the Permafrost ECVs, set by the Global Climate Observing System (GCOS)/World Meteorological Organisation (WMO) are Permafrost temperature, and Thickness of the active layer. The PVIR describes the assessments of three Permafrost_cci products: a) EO-forced simulated Ground Temperature per Depth GTD b) EO-forced simulated Active Layer Thickness ALT and c) Permafrost FRaction PFR derived from GTD at 2 m depth. The validation is carried out independently from the algorithm development team and uses the WMO Global Terrestrial Network for Permafrost (GTN-P), also specifically the mountain permafrost monitoring program PERMOS in Switzerland and additional international and national ground monitoring programs. Standard statistical summaries and binary match-up analyses comparing the in situ measurements with the Permafrost_cci products were used in the validation process. Permafrost_cci also undertakes evaluation experiments in comparing Permafrost_cci permafrost temperature with the spaceborne radar derived Freeze-Thaw to Temperature (FT2T) product and for mountain permafrost areas using in situ ground surface temperature and rockglacier abundance.

Permafrost_cci GTD match-up evaluation between simulated Permafrost_cci and in situ measurements showed the following characteristics: Overall, the simulation dataset had a median Mean Annual Ground Temperature (MAGT) bias of -1.12 °C (95% CI: -4.19 to 2.51 °C). Match-up pairs refined to in situ measurements with MAGT < 1°C and thus from permafrost sites showed a better performance and a median bias of 0.2°C (95% CI: -4.09 to 3.18 °C). Geographically, the extreme residuals showed no obvious spatial clusters. However, a relatively large proportion of residuals >95% quantile were located across Alaska, specifically in the boreal region. Residuals across depths varied around zero, without notable differences in the median bias.

The Permafrost_cci permafrost temperature type (that we defined as GTD < 1°C) showed good performance across the Northern hemisphere, with a median bias of 0.2°C for all depths. Users of Permafrost_cci GTD products should however consider, that Permafrost_cci GTD > 1°C of the discontinuous, sporadic and non-permafrost zones is characterized by a cold median MAGT bias of -1.47 °C. This leads in turn to too shallow simulated Permafost_cci active layer thickness in the permafrost continuous zones around the lower 60 ° Latitudes and an overestimation of the areal extent of permafrost (for Permafrost_cci Permafrost FRraction PFR < 50 %) at the southern boundaries of Permafrost in discontinuous, and sporadic permafrost regions along the southern boundary of permafrost in Eurasia. PERMOS investigations in the Swiss Alps showed in contrast a warm model bias of Permafrost_cci MAGT ranging from +1.22°C at the surface to +1.81°C at 10 m depth with the vast majority of inventoried ESA GlobPermafrost slope movement products located outside of the simulated Permafrost_cci permafrost extent area (Permafrost_cci PFR).

We thus consider Permafrost_cci GTD and PFR products for the Northern hemisphere to be most reliable in the permafrost temperature range with GTD < 1°C and in PFR >50% as well as PFR <14% is reliable as non-permafrost.

1 INTRODUCTION

The European Space Agency (ESA) Climate Change Initiative (CCI) is a global monitoring program with the major aim to provide long-term Earth Observation (EO)-based Essential Climate Variables (ECVs) products serving the climate modelling and climate user communities. Permafrost has been selected as one of the ECVs which are elaborated during Phase 1 of CCI+ (2018-2021). The required parameters for the Permafrost ECVs, set by the Global Climate Observing System (GCOS)/World Meteorological Organisation (WMO) are a) Permafrost temperature, and b) Thickness of the active layer. For the Permafrost_cc product, we added c) Permafrost extent as an additional permafrost parameter; the areal fraction within a pixel that fulfills the definition for the existence of permafrost (ground temperature <0 ºC for two consecutive years).

Validating the CCI product is a critical step to ensure acceptance and correct interpretation of the data by user communities. Here, we provide the validation of the following ECV Permafrost_cci products: i) permafrost temperature, ii) active layer thickness, and iii) permafrost extent. EO-derived permafrost temperature forms the basis to calculate permafrost extent. The calculation of permafrost extent relies on the ground thermal model Permafrost_cci CryoGrid-3 forced by EO-derived Land Surface Temperature (LST) and Snow Water Equivalent (SWE), with boundary conditions of EO-derived Land Cover. A variety of applications and users are expected to benefit from this novel ECV permafrost products, as shown by an extensive user requirement analysis performed at the beginning of the project.

The Committee on Earth Observing Satellites Working Group on Calibration and Validation (CEOS-WGCV) has defined validation as 'the process of assessing the quality of the data products derived from the system outputs, by independent means'. The GEO/CEOS Quality Assurance framework for Earth Observation (QA4EO) provides guidelines for the evaluation of the EO-derived products. GEO/CEOS QA4EO expectations on Fiducial Reference Measurements (FRM) data sets are SI traceability using meteorological standards. However, for several geoscientific EO applications, accuracy can only be measured in terms of an agreement, or in terms of omission and commission errors. Therefore, if validation against precise FRM according to QA4EO criteria is not feasible, evaluation against suitable in situ measurements or against other sources using expert knowledge is acceptable. According to QA4EO-criteria, validation needs to be independent from the retrieval process of the product. In the QA4EO sense, suitable validation data sets are characterised by measurement protocols and community-wide management practices and published openly. The validation data collection shall be a part of a collaborative user environment within an international framework. Within the Permafrost_cci validation framework we guarantee independent validation, carried out with strong support of the user communities. WMO and GCOS delegated the global monitoring of the ECV Permafrost to the Global Terrestrial Network for Permafrost (GTN-P) that is managed by the International Permafrost Association (IPA). GTN-P/IPA established the Thermal State of Permafrost Monitoring (TSP) for permafrost temperature monitoring and the Circumpolar Active Layer Monitoring program (CALM) for active layer thickness monitoring. Both GTN-P monitoring programs, TSP and CALM, require community standards for measurements and data collection and publish data sets (Biskaborn et al. 2015, 2019). The collected in situ measurements in the GTN-P monitoring programs, TSP and CALM, and other international and national climatological and meteorological measurement programs are characterised by community-wide management, best practices with open data access, and a collaborative user environment within an international framework: This document provides the validation and intercomparison results of the Permafrost_cci permafrost temperature, active layer depth and permafrost extent products.

1.1 Purpose of the Document

The PVIR describes the assessments to evaluate the Climate Research Data Package CRDP Permafrost_cci products. Besides the required parameters of a) permafrost temperature, and b) active layer thickness, Permafrost_cci provides c) Permafrost extent (Permafrost fraction within a pixel), as an additional variable derived from Permafrost temperature: the areal fraction within an area (pixel) that fulfills the definition for the existence of permafrost (ground temperature <0 ºC for two consecutive years).

The generation of depth-specific ground temperature and thaw-depth time series relies on the ground thermal model Permafrost_cci CryoGrid 3, that is forced by EO-derived time series of LST and SWE with boundary conditions of EO-derived Land Cover. The Permafrost_cci CRDPv2 released in 2021 includes three time series covering the Northern Hemisphere north of 30° N:

- simulated EO-forced mean annual Ground Temperature per Depth (GTD) in 5 discrete depths (0 m, 1 m, 2 m, 5 m, 10 m) from 1997 to 2019
- simulated EO-forced Active Layer Thickness (ALT) from 1997 to 2019
- Permafrost FRaction (PFR) derived from GTD from 1997 to 2019.

The PVIR version- 3 assesses the Permafrost_cci products GTD, ALT and PFR in lowlands and mountain permafrost regions north of 30° N.

1.2 Structure of the Document

The PVIR is organised in 6 chapters.

- Chapter 1 provides the introduction and the overview on Permafrost_cci including applicable documents and the community glossary for Permafrost.
- Chapter 2 and its subsections describe the reference data sets and methods for the assessment of the variables: permafrost temperature, active layer thickness and permafrost extent.
- Chapters 3, 4, 5 present the results of the quality assessment for the Permafrost_cci products:
  - o Chapter 3 describes the quality assessment for Permafrost_cci permafrost temperature
  - o Chapter 4 describes the quality assessment for Permafrost_cci active layer thickness
  - o Chapter 5 describes the quality assessment for Permafrost_cci permafrost extent
- Chapter 6 provides a summary and recommendations.

1.3 Applicable Documents

[AD-1] ESA 2017: Climate Change Initiative Extension (CCI+) Phase 1 New Essential Climate Variables - Statement of Work. ESA-CCI-PRGM-EOPS-SW-17-0032

[AD-2] Requirements for monitoring of permafrost in Polar Regions - A community white paper in response to the WMO Polar Space Task Group (PSTG), Version 4, 2014-10-09. Austrian Polar Research Institute, Vienna, Austria, 20 pp

[AD-3] ECV 9 Permafrost: assessment report on available methodological standards and guides, 1 Nov 2009, GTOS-62

[AD-4] GCOS-200, the Global Observing System for Climate: Implementation Needs (2016 GCOS Implementation Plan, 2015

1.4 Reference Documents

[RD-1] Bartsch, A., Grosse, G., Kääb, A., Westermann, S., Strozzi, T., Wiesmann, A., Duguay, C., Seifert, F.M., Obu, J., Goler, R. (2016): GlobPermafrost – How space-based earth observation supports understanding of permafrost. Proceedings of the ESA Living Planet Symposium, pp. 6.

[RD-2] Bartsch, A., Westermann, Strozzi, T., Wiesmann, A., Kroisleitner, C. (2020): ESA CCI+ Permafrost Product Specifications Document, v2.0

[RD-3] Bartsch, A., Matthes, H., Westermann, S., Heim, B., Pellet, C., Onacu, A., Kroisleitner, C., Strozzi, T. (2020): ESA CCI+ Permafrost User Requirements Document, v2.0

[RD-4] Heim, B., Wieczorek, M., Pellet, C., Barboux, C., Delaloye, R., Bartsch, A, Strozzi, T. (2020): ESA CCI+ Product Validation Plan, v2.0

[RD-5] Bartsch, A., Westermann, S., Heim, B., Wieczorek, M., Pellet, C., Barboux, C., Kroisleitner, C., Strozzi, T. (2019): ESA CCI+ Permafrost Data Access Requirements Document, v1.0

[RD-6] Heim, B., Wieczorek, M., Pellet, C., Barboux, C., Delaloye, R., Bartsch, A., Strozzi, T. (2019): ESA CCI+ PVIR, v1.0

[RD-7] Heim, B., Wieczorek, M., Pellet, C., Delaloye, R., Barboux, C., Westermann, S., Bartsch, A, Strozzi, T. (2020): ESA CCI+ Product Validation Plan, v2.0

1.5 Bibliography

A complete bibliographic list that support arguments or statements made within the current document is provided in Section 7.1.

1.6 Acronyms

A list of acronyms is provided in section 7.2.

1.7 Glossary

The list below provides a selection of terms relevant for the parameters addressed in Permafrost_cci [AD-1]. A comprehensive glossary is available as part of the Product Specifications Document [RD-2].

active-layer thickness

The thickness of the ground layer that is subject to annual thawing and freezing above permafrost.

The thickness of the active layer depends on factors such as the ambient air temperature, vegetation, drainage, soil or rock type and total water content, snowcover, and degree and orientation of slope. As a rule, the active layer is thin in the High Arctic (it can be less than 15 cm) and becomes thicker farther south (1 m or more).

The thickness of the active layer can vary from year to year, primarily due to variations in the mean annual air temperature, distribution of soil moisture, and snowcover.

The thickness of the active layer includes the uppermost part of the permafrost wherever either the salinity or clay content of the permafrost allows it to thaw and refreeze annually, even though the material remains cryotic (T <0 °C).

Use of the term "depth to permafrost" as a synonym for the thickness of the active layer is misleading, especially in areas where the active layer is separated from the permafrost by a residual thaw layer, that is, by a thawed or noncryotic (T >0 °C) layer of ground.

REFERENCES: Muller, 1943; Williams, 1965; van Everdingen, 1985

continuous permafrost

Permafrost occurring everywhere beneath the exposed land surface throughout a geographic region with the exception of widely scattered sites, such as newly deposited unconsolidated sediments, where the climate has just begun to impose its influence on the thermal regime of the ground, causing the development of continuous permafrost.

For practical purposes, the existence of small taliks within continuous permafrost has to be recognized. The term, therefore, generally refers to areas where more than 90 percent of the ground surface is underlain by permafrost.

REFERENCE: Brown, 1970.

discontinuous permafrost

Permafrost occurring in some areas beneath the exposed land surface throughout a geographic region where other areas are free of permafrost.

Discontinuous permafrost occurs between the continuous permafrost zone and the southern latitudinal limit of permafrost in lowlands. Depending on the scale of mapping, several subzones can often be distinguished, based on the percentage (or fraction) of the land surface underlain by permafrost, as shown in the following table.

Permafrost	English usage	Russian Usage
Extensive	65-90%	Massive Island
Intermediate	35-65%	Island
Sporadic	10-35%	Sporadic
Isolated Patches	0-10%	-

SYNONYMS: (not recommended) insular permafrost; island permafrost; scattered permafrost.
REFERENCES: Brown, 1970; Kudryavtsev, 1978; Heginbottom, 1984; Heginbottom and Radburn, 1992; Brown et al., 1997.

mean annual ground temperature (MAGT)

Mean annual temperature of the ground at a particular depth.
The mean annual temperature of the ground usually increases with depth below the surface. In some northern areas, however, it is not un-common to find that the mean annual ground temperature decreases in the upper 50 to 100 metres below the ground surface as a result of past changes in surface and climate conditions. Below that depth, it will increase as a result of the geothermal heat flux from the interior of the earth. The mean annual ground temperature at the depth of zero annual amplitude is often used to assess the thermal regime of the ground at various locations.

permafrost

Ground (soil or rock and included ice and organic material) that remains at or below 0°C for at least two consecutive years.
Permafrost is synonymous with perennially cryotic ground: it is defined on the basis of temperature. It is not necessarily frozen, because the freezing point of the included water may be depressed several degrees below 0°C; moisture in the form of water or ice may or may not be present. In other words, whereas all perennially frozen ground is permafrost, not all permafrost is perennially frozen. Permafrost should not be regarded as permanent, because natural or man-made changes in the climate or terrain may cause the temperature of the ground to rise above 0 °C.
Permafrost includes perennial ground ice, but not glacier ice or icings, or bodies of surface water with temperatures perennially below 0°C; it does include man-made perennially frozen ground around or below chilled pipe-lines, hockey arenas, etc.
Russian usage requires the continuous existence of temperatures below 0 °C for at least three years, and also the presence of at least some ice.
SYNONYMS: perennially frozen ground, perennially cryotic ground and (not recommended) biennially frozen ground, climafrost, cryic layer, permanently frozen ground.
REFERENCES: Muller, 1943; van Everdingen, 1976; Kudryavtsev, 1978.

2 METHODS FOR QUALITY ASSESSMENT

This chapter provides an overview of methods used to evaluate the performance of the Permafrost_cci products. The Permafrost_cci products will be analysed and discussed in the following order: Permafrost_cci mean annual Ground Temperature per Depth (GTD), Active Layer Thickness (ALT) and Permafrost Fraction (PFR) [RD-3]. In the validation process, we compiled a substantial in situ data collection from international and national permafrost and climate data monitoring networks and cooperation with the permafrost community plays a central role.

The majority of the in situ data collection described in [RD-5] is contributed from the WMO-GCOS Global Terrestrial Network for Permafrost GTN-P of the International Permafrost Association (IPA) and the national-wide Russian meteorological monitoring network ROSHYDROMET (RHM) program. GTN-P and ROSHYDROMET time series and data collections from additional networks provide ground-based measured reference data sets. All these measurement series are no easy-to-use or readily available time-series data that are data-fit for validation and round robin exercises. For example, the data collection of ground-temperature time series is a highly complex and heterogeneous data set including variable timeframes from hourly over annually to sporadic measurements, in different depths and not consistent over time. In addition, all the available published in situ data sets contained a large amount of caveats, including erroneous or imprecise coordinate locations, depending on region and Principal Investigators (PIs). Within Permafrost_cci, the pre-existing community in situ data have been error-checked, corrected, homogenised, filtered and standardised. The newly compiled, harmonised Permafrost_cci set of ground temperature depth-time series provides the first consistent reference data set usable for evaluation of ground temperature in the circum-Arctic. It covers all permafrost zones from continuous to discontinuous, sporadic and isolated of the Northern Hemisphere with all available measurement depths down to 20 m.

The Permafrost_cci products are evaluated using pixel-based match-up analyses. On one hand, the assembled Permafrost_cci in situ reference data collections of MAGT and ALT are characterised by spatial and temporal biases related to regions, time covered and measurement depths due to the high variety in national measurement programs, PIs and funding sources. On the other hand, we are facing a spatial-scale mismatch between in situ measurements, i.e., the borehole locations or the 100 m×100 m CALM grid measurements versus the coarse-scale Permafrost-cci grid cells. Already with the MODIS-derived sinusoidal geometry, each location of a situ measurement is moved further away from its original location to a nearby location on the grid. In addition, the Polar stereographic projection that is finally applied requires pixel infilling and further smooths out landscape heterogeneity. The comparison of shallow depths further compromises the precision, as permafrost landscapes may contain heterogeneous micro-topography, leading to an inconsistent depth extrapolation for shallow depths. Despite these challenges, the Permafrost_cci match-up analyses do provide the estimation of the accuracy and usability of the Permafrost_cci products.

Specifically, for mountain permafrost, GTN-P PERMOS in Switzerland assessed the Permafrost_cci permafrost temperature and permafrost extent products, using in situ observations of surface temperature and borehole ground temperatures and the ESA GlobPermafrost rock glacier inventory.

For a cross-product assessment we applied the Freeze-Thaw to Temperature (FT2T) product, an space-borne radar-derived ground temperature product, for comparison with the Permafrost_cci permafrost temperature product.

Permafrost_cci entirely acknowledges the efforts of the international permafrost community in this impressive realization of circumpolar measurements, and all national initiatives from Russia, US, Canada, Switzerland and Norway for making the measurement data publicly available. The match-up dataset and its characteristics as well as data sources and availability are described in detail in the Permafrost_cci DARD [RD-5] and PVP [RD-4] reports. The previous product quality assessments are described in the PVIRs v1 [RD-76] and v2 [RD-7].

2.1 Pair-wise Match-up Evaluation

We constructed a pixel-based pairwise Permafrost_cci match-up data collection based on

i) in situ data time series. This data collection presents a novel standardised data set from diverse community data archives across all permafrost zones (continuous, discontinuous, sporadic, and isolated).

- in situ MAGT [Latitude, Longitude] in discrete depths in annual resolution from 1997 to 2019
- in situ PFR [Latitude, Longitude] permafrost probability in annual resolution from 1997 to 2019
- in situ ALT [Latitude, Longitude] in annual resolution from 1997 to 2019

ii) Permafrost_cci CRDPv2 ECV time series on MAGT at discrete ground depths (0, 1, 2, 5, 10 m), Active Layer Thickness (ALT) and Permafrost Extent (PFR; permafrost probability) in polar stereographic projection with 1 km grid cell resolution. The Match up analyses in this study include linearly interpolated depths at the locations of the in situ measurements.

- Permafrost_cci GTD (=MAGT) [Latitude, Longitude] in discrete depths (0, 0.2, 0.25, 0.4, 0.5, 0.6, 0.75, 0.8, 1.0, 1.2, 1.6, 2.0, 2.4, 2.5, 3.0, 3.2, 4.0, 5.0, 10.0, 20.0 m) in annual resolution from 1997 to 2019.
- Permafrost_cci ALT [Latitude, Longitude] in annual resolution from 1997 to 2019.
- Permafrost_cci PFR [Latitude, Longitude] permafrost probability (extracted at 2 m depth) in annual resolution from 1997 to 2019.

Permafrost_cci undertakes the pixel-based comparison between the simulated Permafrost_cci products MAGT, ALT and PFR products and in situ measurements at individual stations relying on statistical metrics for its common usage.

2.2 Assessment of Permafrost Temperature

2.2.1 Ground Temperature Reference Data

A major data provider for ground temperature time series is the WMO/GCOS **Global Terrestrial Network for Permafrost GTN-P** (https://gtnp.arcticportal.org/), the global permafrost monitoring program of the International Permafrost Association IPA. Compiled GTN-P and United States Geological Survey USGS data are also published in the Arctic Data Center (US) (https://arcticdata.io/catalog/#view/doi:10.18739/A2KG55; Wang et al. 2018). Several more important GTN-P collections and data from individual members of the Permafrost research community are published in the PANGAEA data repository for environmental research (DE) (https://doi.pangaea.de/10.1594/PANGAEA.905233; Boike

et. al. 2019; https://doi.pangaea.de/10.1594/PANGAEA.884711, GTN-P 2018), https://doi.pangaea.de/10.1594/PANGAEA.912482, Bergstedt & Bartsch 2020). In addition, we received ground data from more individual members of the Permafrost research community (PIs V. Romanovski and A. Kholodov (GTN-P, University of Alaska Fairbanks, US), PI M. Ulrich (University of Leipzig, DE) connected to GTN-P but not yet with these data published within the GTN-P data repository frameworks. Therefore, within our reference data collection these data are also named GTN-P. Further relevant data providers are the WMO **Roshydromet RHM** national hydrometeorological monitoring program for Russia (http://meteo.ru/data/164-soil-temperature), **Nordicana-D,** the Canadian data repository for Polar research, http://www.cen.ulaval.ca/nordicanad/dpage.aspx?doi=45291SL34 F28A9491014AFD; Allard et al., 2016, CEN 2013) and the **NASA Arctic-Boreal Vulnerability Experiment ABoVE** https://above.nasa.gov/field_data_products.html.

[RD-5] describes the data sources, measurement programs and the data compilation steps in detail. We undertook coordinate corrections, outlier and error elimination. We also processed shallow and deep depth profiles with two different processing steps: For shallow Ground Temperature GT depth profiles down to 5 m depth, all discrete values were calculated. For GT depth profiles of 5 m depth and deeper, we discard all data <2 m depth as in boreholes with large diameters, there is frequently artificial material in-filling or air. Data <2 m were only kept if confirmed reliable by the PI.

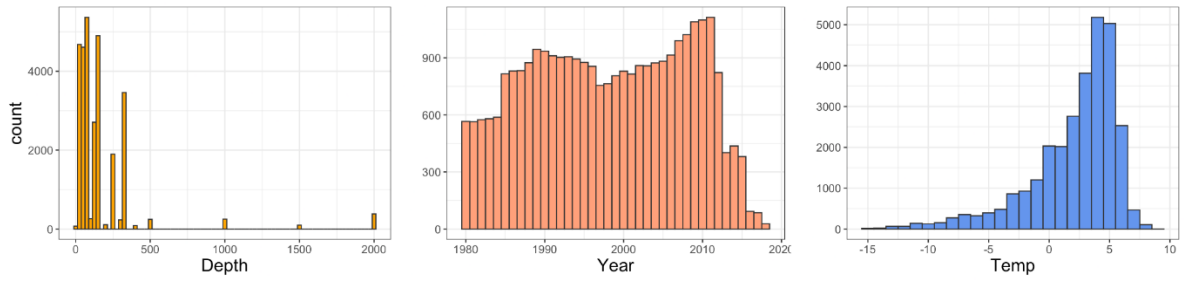

Figure 2.1: Sample size of complete in situ dataset of mean annual ground temperatures (MAGT) at discrete depths (left), for the years 1980 to 2019 (center), and across temperatures (right).

The Permafrost_cci reference data consists of standardised mean annual Ground Temperature per Depth GTD from 1980 to 2019 (Figure 2.1), with product depths at 0, 0.2, 0.25, 0.4, 0.5, 0.6, 0.75, 0.8, 1.0, 1.2, 1.6, 2.0, 2.4, 2.5, 3.0, 3.2, 4.0, 5.0, 10.0, 15.0, 20.0 m. The reference data also holds metadata information, which allows assessing the quality of each temperature value (Table 2.1). These metadata comprise for yearly values the ratio of missing data per month/year (missing days per year/365) and the amount of completely missing months. Yearly means are not calculated if >20% of yearly values are not available or if more than one complete month is missing. An exception is made for data at the depth of Zero Annual Amplitude (ZAA).

This Permafrost_cci GT match-up data collection v3 contains data from 354 in situ measurement locations (GTN-P and USGS n = 2,831, RHM n = 10,929, Nordicana-D n = 322, NASA ABoVE n = 25), with overall n =14,107 match-up pairs in time and depth (Figure 2.2, 2.3). The Permafrost_cci GT match-up data collection v3 < 1 °C contains data from 234 in situ measurement locations (Figure 2.4) with overall n =4,672 match-up pairs in time and depth.

Table 2.1. Example of how the compiled data set provides metadata information of yearly values across depths. Mxx = ratio of missing values per month/year at depth xx m. mMxx = number of completely missing months per year at depth xx m.

Site	Year	Type	M0	M0.2	M0.25	M0.4	M0.5	M0.75	M0.8	M1	mM0	mM0.2	mM0.2	mM0.4	mM0.5	mM0.7	mM0.8	mM1	0	0.2	0.25	0.4	0.5	0.75	0.8	1
FB_dry_l	2006	Mean	1	1	1	1	1	1	1	1	12	12	12	12	12	12	12	12	NA	NA	NA	NA	NA	NA	NA	NA
FB_dry_l	2006	Max	1	1	1	1	1	1	1	1	12	12	12	12	12	12	12	12	NA	NA	NA	NA	NA	NA	NA	NA
FB_dry_l	2006	Min	1	1	1	1	1	1	1	1	12	12	12	12	12	12	12	12	NA	NA	NA	NA	NA	NA	NA	NA
FB_wet_	2006	Mean	0.414	0.414	0.414	0.416	0.414	NA	NA	NA	5	5	5	5	0	NA	NA	NA	1.33	1.64	1.56	1.35	1.12	NA	NA	NA
FB_wet_	2006	Max	0.414	0.414	0.414	0.416	0.414	NA	NA	NA	5	5	5	5	0	NA	NA	NA	18.9	12.7	12	10.4	8.07	NA	NA	NA
FB_wet_	2006	Min	0.414	0.414	0.414	0.416	0.414	NA	NA	NA	5	5	5	5	0	NA	NA	NA	-19.1	-12	-11.5	-10.2	-8.95	NA	NA	NA
FB_dry_l	2007	Mean	0.581	0.581	0.581	0.581	0.581	1	0.586	0.699	7	7	7	7	7	12	7	8	-3.58	-2.65	-2.53	-2.38	-2.44	NA	-2.4	-2.59
FB_dry_l	2007	Max	0.581	0.581	0.581	0.581	0.581	1	0.586	0.699	7	7	7	7	7	12	7	8	13.6	10.4	9.31	8.01	4.87	NA	1.73	0.63
FB_dry_l	2007	Min	0.581	0.581	0.581	0.581	0.581	1	0.586	0.699	7	7	7	7	7	12	7	8	-21.9	-17.5	-16.9	-16	-14.6	NA	-11.9	-8.83
FB_wet_	2007	Mean	0	0	0	0	0	NA	NA	NA	0	0	0	0	0	NA	NA	NA	-5.99	-5.41	-5.62	-5.48	-5.63	NA	NA	NA
FB_wet_	2007	Max	0	0	0	0	0	NA	NA	NA	0	0	0	0	0	NA	NA	NA	17.8	15.2	11.7	10.6	7.49	NA	NA	NA
FB_wet_	2007	Min	0	0	0	0	0	NA	NA	NA	0	0	0	0	0	NA	NA	NA	-30.2	-23.3	-22.7	-21.3	-20.3	NA	NA	NA
FB_dry_l	2008	Mean	0.18	0.18	0.18	0.18	0.18	1	0.183	0.183	2	2	2	2	2	12	2	2	-7.37	-6.62	-6.63	-6.63	-6.44	NA	-6.26	-5.82
FB_dry_l	2008	Max	0.18	0.18	0.18	0.18	0.18	1	0.183	0.183	2	2	2	2	2	12	2	2	18.7	13.2	11.8	9.48	8.1	NA	3.79	1.35
FB_dry_l	2008	Min	0.18	0.18	0.18	0.18	0.18	1	0.183	0.183	2	2	2	2	2	12	2	2	-28.7	-23.9	-23.2	-22.4	-20.7	NA	-18.2	-15.1
FB_wet_	2008	Mean	0.372	0.372	0.372	0.426	0.372	NA	NA	NA	4	4	5	4	0	NA	NA	NA	-6.62	-7.34	-7.43	-9.01	-7.73	NA	NA	NA
FB_wet_	2008	Max	0.372	0.372	0.372	0.426	0.372	NA	NA	NA	4	4	5	4	0	NA	NA	NA	18.2	12.4	11.8	9.71	9.12	NA	NA	NA
FB_wet_	2008	Min	0.372	0.372	0.372	0.426	0.372	NA	NA	NA	4	4	5	4	0	NA	NA	NA	-24.9	-22	-21.7	-20.7	-20.2	NA	NA	NA
FB_dry_l	2009	Mean	0.586	0.003	0	0.586	0	0.414	0.586	0.586	7	0	0	7	0	5	7	7	-13.2	-3.73	-3.9	-11.5	-3.92	0.11	-9.42	-7.8
FB_dry_l	2009	Max	0.586	0.003	0	0.586	0	0.414	0.586	0.586	7	0	0	7	0	5	7	7	-1.34	13.5	11.5	-3.74	7.1	3.58	-2	-1.09
FB_dry_l	2009	Min	0.586	0.003	0	0.586	0	0.414	0.586	0.586	7	0	0	7	0	5	7	7	-19.9	-18	-17.7	-17.3	-16.2	-5.97	-14.3	-11.9
FB_wet_	2009	Mean	0.414	0.416	0.416	1	0.414	NA	NA	NA	5	5	12	5	0	NA	NA	NA	1.95	1.65	1.65	NA	1.46	NA	NA	NA

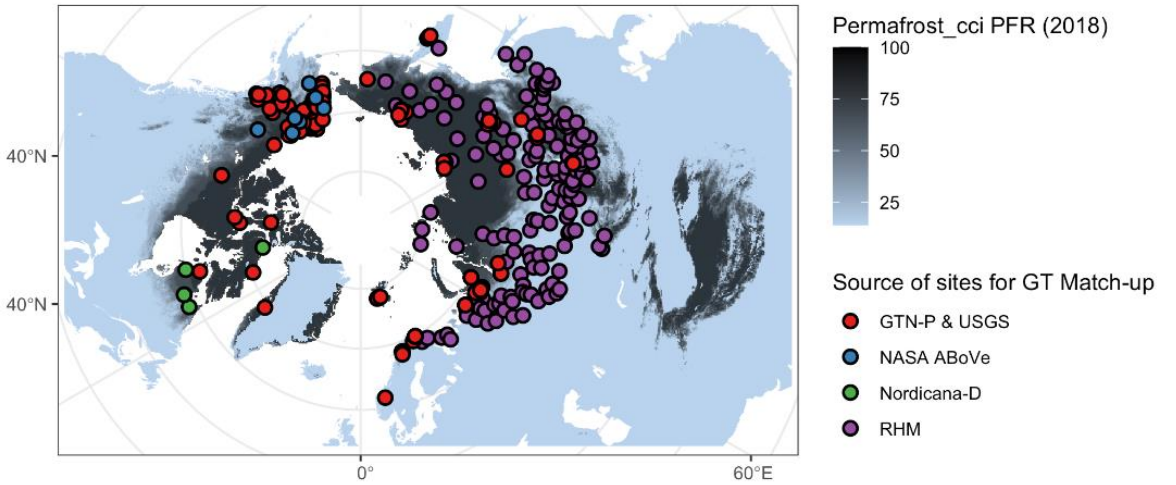

Figure 2.2. Northern hemisphere Permafrost_cci PFR permafrost probability and in situ ground temperature stations (grouped by data source).

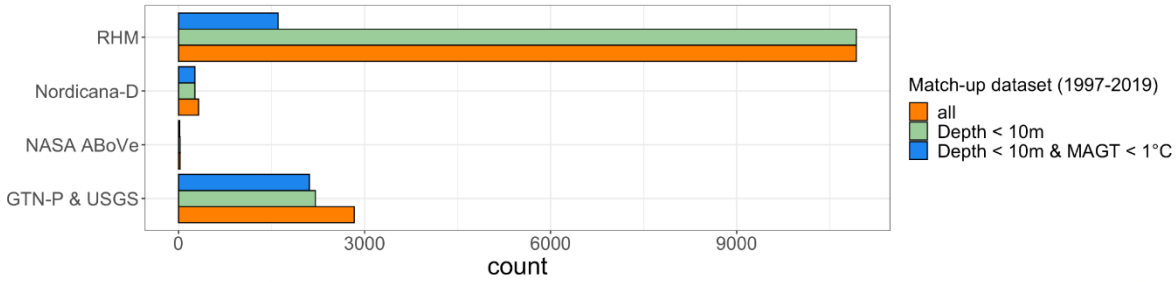

Figure 2.3. Sample size of in situ MAGT match-up dataset grouped by data source.

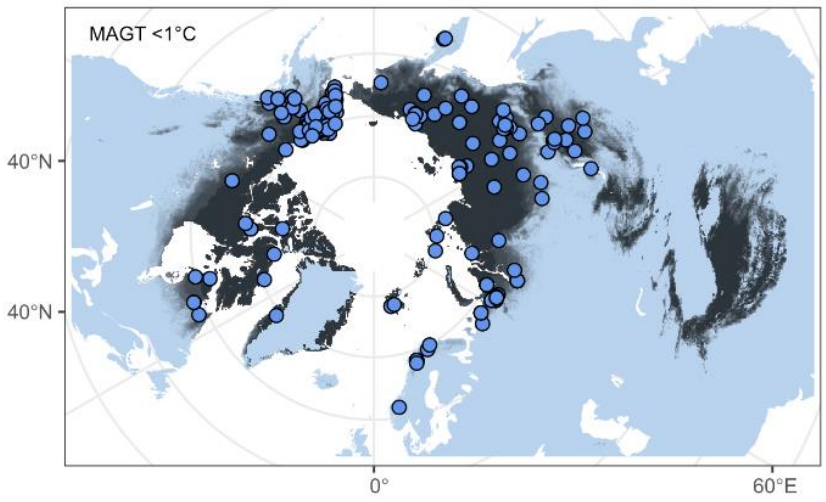

Figure 2.4 Northern hemisphere Permafrost_cci PFR permafrost probability and in situ ground temperature stations with MAGT <1 °C (n sites = 234, n samples = 4,672)

Versions of Ground Temperature Reference and Match-up Data Sets

Exclusion of non-permafrost temperatures in GTD match-up Data Set v1 (Validation in phase 1, CRDPv0 2019)

For straightforward match-up analyses in the first validation round [RD-7], we focused on the permafrost temperature range excluding all stations with in situ measurements of MAGT ≥1 °C at least once (independent of measurement depth) from the match-up analyses. This GTD match-up dataset, with all 'warm temperature' station types excluded, contained n = 3,185 pairs in time and depth.

Inclusion of warm temperatures, exclusion of Yedoma regions in Siberia in GTD match-up Data Set v2 (Validation in phase 2, CRDPv1 2020)

We conducted the validation version 2 using the GTD data collection with MAGT ≥1 °C included (depths down to 10 m). This GTD match-up data set for Permafrost_cci MAGT in 0, 0.2, 0.25, 0.4, 0.5, 0.6, 0.75, 0.8, 1.0, 1.2, 1.6, 2.0, 2.4, 2.5, 3.0, 3.2, 4.0, 5.0, 10.0 m depth included n = 13,695 match-up pairs in time and depth from n = 300 sites.

As especially the Russian boreholes have only few measurements at exactly 1 or 2 m depth, we interpolated temperature values for the Permafrost_cci product depths. To achieve this, we only use sites with at least three sensors in the lower depth down to 1.20 m. Interpolation was conducted by linear regression between two single measurement depths, resulting in separate equations for each sensor-pair and year.

Please note that we excluded all sites that are not representative of the landscape-scale of in situ measurements from all three match-up data collections: these are selected mountain sites (n = 18) that are specifically assessed by PERMOS, small-scale landscape anomalies such as very local peatland patches or in situ measurements in pingos (ice hills, n = 3). Please also note that we excluded all sites within the Siberian Yedoma area (shape file from Bryant et al., 2017) due to incorrect parameterisation of Yedoma stratigraphy (n = 7) in *CRDPv1*.

GT match-up Data Set v3 (Validation in phase 3, CRDPv2 2021)

We conduct the validation version 3 using the GTD data collection with interpolated depths down to 20 m. This GTD match-up data set for Permafrost_cci MAGT in 0, 0.2, 0.25, 0.4, 0.5, 0.6, 0.75, 0.8, 1.0, 1.2, 1.6, 2.0, 2.4, 2.5, 3.0, 3.2, 4.0, 5.0, 10.0, 20.0 m depth includes n = 14,107 match-up pairs in time and depth from 354 sites.

The PERMOS mountain permafrost sites and landscape anomalies excluded in version 2 were also excluded in this version 3. All sites within the Siberian Yedoma area are included in version 3 as *CRDPv2* contains no artefacts in the Yedoma regions.

2.2.2 Characteristics of Ground Temperature Match-up Data Set

The GTD match-up v3 (2021) contains the cleaned and interpolatd in situ MAGT at discrete depths matched with interpolated CRDPv2 Permafrost_cci MAGT at 0, 0.2, 0.25, 0.4, 0.5, 0.6, 0.75, 0.8, 1.0, 1.2, 1.6, 2.0, 2.4, 2.5, 3.0, 3.2, 4.0, 5.0, 10.0, 20.0 m depth. Figure 2.5 shows the frequency distribution of the Match up data with n = 14,107, Figure 2.7 with in situ MAGT ≥1 °C excluded, with n = 4,672.

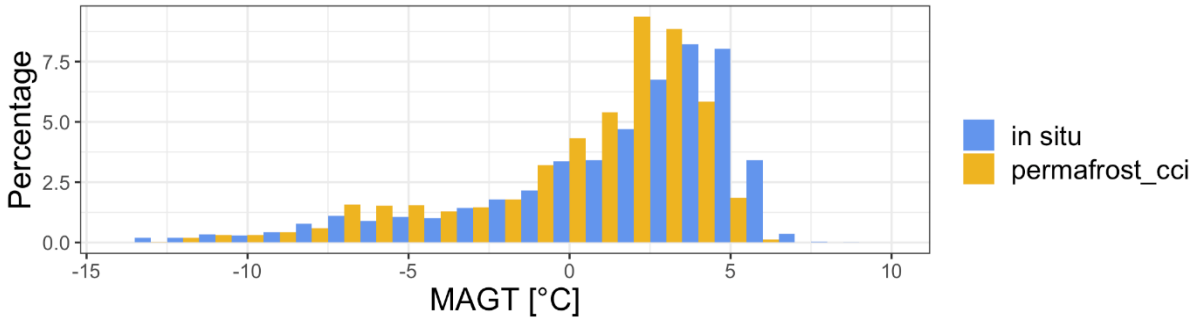

Figure 2.5. Frequency distribution of the match-up data collection v3, at all discrete depths ≤10 m in entire ranges with steps of 1 °C, n = 14,107.

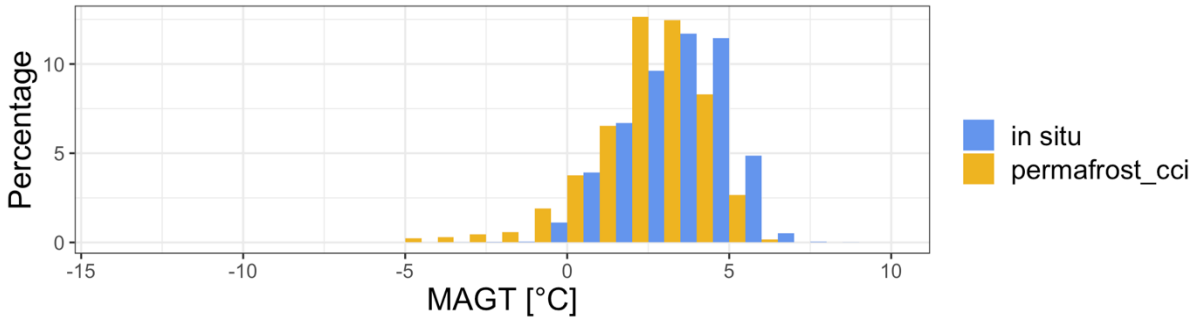

Figure 2.6. Frequency distribution of the match-up data collection v3with MAGT ≥1 °C excluded, n = 4,672 (excluded samples = 9427). The match-up data characteristics of MAGT (Figure 2.6) show a frequency distribution skewed towards the cold temperature range with the highest number of samples in the warm temperature range >0 °C.

The MAGT sample size peaks between 3 and 4 °C for Permafrost_cci MAGT and between 4 and 5 °C for in situ MAGT. This data group is mainly constructed from the RHM long-term measurement network. The frequency distribution for the MAGT match-up < 1°C (Figure 2.6). The depth-specific frequency distributions vary as they cover different latitudes and regions depending on the data provider. RHM with main contributions to depths of 0.80, 1.20, 2.40 m covers fewer measurement sites at high

latitudes than GTN-P and Nordicana-D that more frequently cover the depths of 0.75, 1.00 and 2.00 m (Figure 2.7).

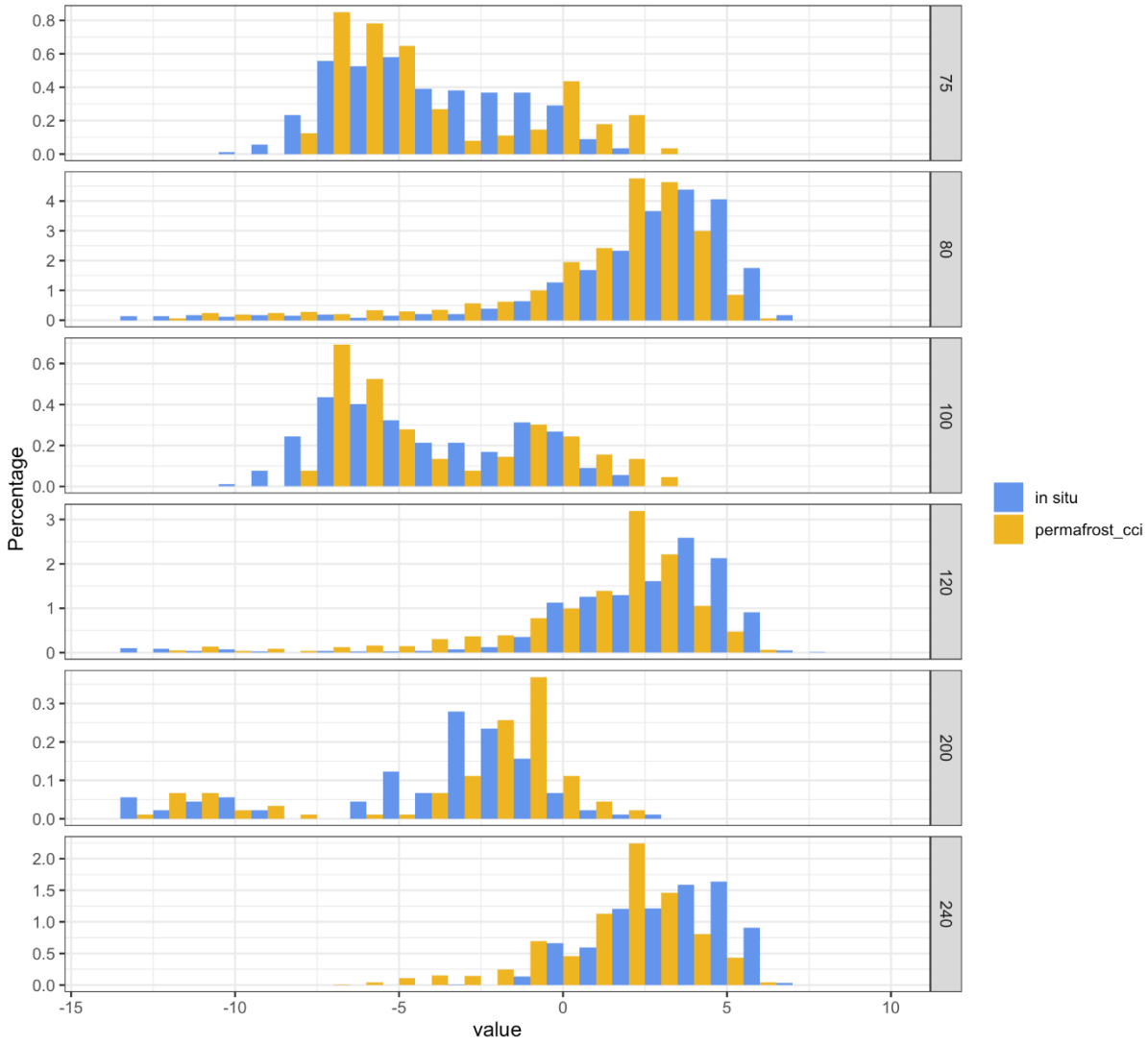

Figure 2.7. Frequency distribution of the match-up data collection v3 confined to match-up pairs in specific ground temperature sensor depths (0.75, 0.80, 100, 120, 200, 240 cm).

2.2.3 PERMOS Reference GST and GTD data generation

The PERMOS network currently comprises 27 boreholes distributed within 16 sites (Figure 2.13) across Switzerland, which continuously measure permafrost temperatures between 0 and 100 m depth. The sites are located at elevations between 2400 m a.s.l. and 3400 m a.s.l. with boreholes drilled in bedrock, rock glaciers, talus slopes, steep rock walls or moraines ([RD-5], Table 4.4).

For each single borehole, PERMOS selected the thermistor closest to the depth of the Permafrost_cci GTD POL product (0, 1, 2, 5 and 10 m) and compiled mean annual ground temperature (MAGT) over the period 1997-2019. Only data series with at least 80% data completeness over the year were selected for computing MAGT.

The match-up of the 1 km x 1 km grid cell of the Permafrost_cci product with the in situ data functions by selecting the grid cells in which the boreholes are located. The in situ measured and Permafrost_cci simulated MAGT values are compared pairwise for each single borehole and depth. In mountainous terrains, the differences in the subsurface thermal regime due to varying climate conditions (i.e. latitudinal and regional gradient) are considered smaller than those caused by topography or surface and subsurface conditions of the different landforms. Therefore, we analysed the model performance based on the landform typologies rather than based on climatic regions.

Ground surface temperature (GST) are temperatures measured between 0 and 10 cm depth by miniature loggers placed only with a small distance below the surface to avoid the influence of the direct shortwave radiation and to capture a slightly filtered temperature signal. Within the PERMOS network, GST are measured at 23 different sites, each with 4 to more than 20 individual loggers adding up to 247 measurement points (see also Figure 2.13). Each logger measures continuously with a temporal resolution of 1 to 3 hours.

Based on this data set, PERMOS computed mean annual ground surface temperature (MAGST) for each single logger over the period 1997 to 2019. Only series with at least 80% data completeness over the year were selected for computing the annual mean. Thus, the number of MAGST available is variable from one year to the next. It ranges from 16 MAGST match-up data computed in 1997 to 242 in 2011.The MAGST data is highly variable depending on snow conditions, radiation and shading effects as well as surface and subsurface properties. The variability within one specific site (i.e., 4 to 30 loggers) was found to be in the same range as the variability in-between the different sites.

Given the high impact of topography and other (sub-)surface properties on the GST, a direct match-up between the 1 km x 1 km grid cell of the Permafrost_cci GTD product and single point locations is inapplicable. Therefore, we computed the average MAGST of all available GST logger and compared it to the average of all Permafrost_cci GT grid cells located between 2500 and 3000 m a.s.l.

2.2.4 Satellite derived Freeze/Thaw Surface Status GT evaluation data set generation

The Freeze-Thaw to Temperature (FT2T) model is an empirical model, based on a linear regression analysis between the annual sum of frozen days, measured with microwave EO sensors, and in situ ground temperature measurements (Kroisleitner et al., 2018). It was initially developed for temperature retrieval at coldest sensor depth spanning the years 2007-2013 available from Paulik et al. (2014). The method by Naeimi et al. (2012) which forms the basis for the 2007-2013 record of Paulik et al. (2014) has been applied to further records, extending the dataset to 2018. The method and set parameters were evaluated by in situ records and C-band SAR data (Sentinel-1; Bergstedt et al. 2020b). A Metop ASCAT global gridded data set available from EUMETSAT (SOMO12) has been used for this purpose. FT2T has been further developed for Permafrost_cci to represent the depths of the CRDPv2 and calendar years. With respect to in situ data availability for the model calibration, only 1 m depth can be considered. Further improvements have been made regarding bias correction for lake fraction using Sentinel-1 (Bergstedt et al., 2020a). These apply to lake rich regions. Records have been extracted for selected borehole locations of the match-up data set for site comparisons and for regions in addition to the circumpolar comparison presented in [RD-6].

2.3 Assessment of Active Layer Thickness

2.3.1 Active Layer Thickness Reference Data

Same as for permafrost temperature, the major data provider for ALT time series is the WMO/GCOS Global Terrestrial Network for Permafrost GTN-P, the global permafrost monitoring programme of the International Permafrost Association IPA. The comprehensive, continuously updated GTN-P data collection of ALT time series is available for download under the Circum-Polar Active Layer Monitoring Network, https://www2.gwu.edu/~calm/. [RD-5] describes the CALM measurement program and the data compilation steps in detail. For an in situ estimation of ALT, it is relevant to measure active layer depths at the end of the active-layer thawing season in late summer. This maximum thaw depth measured in late summer represents the ALT of a specific year. For some measurements in the CALM ALT data collection, metadata information indicates that a value was measured earlier in summer during a year. These active layer depth measurements, not representing the Permafrost ECV ALT, were discarded. Figure 2.8 shows an overview on the CALM measurement network of the Northern hemisphere including the measurement sites in Mongolia, central Asia and in China on the Tibetan plateau.

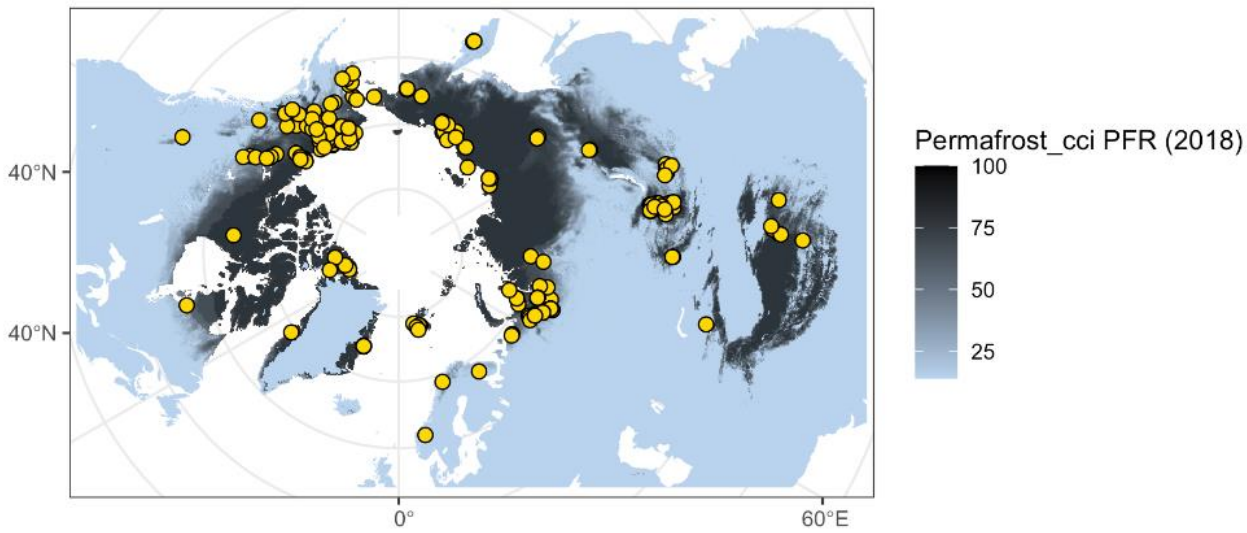

Figure 2.8. Northern hemisphere Permafrost_cci PFR permafrost probability and in situ sites (yellow symbols) of active layer depth ALT (GTN-P CALM programme).

Versions of ALT and Match-up Data Sets

Version 1 ALT Match up collection (2003 to 2017) (Validation in phase 1, CRDPv0 2019)

standardised annual ALT time series from 2003 and 2017 with a circum-Arctic geographic coverage. The collection contained data from 207 sites (China + Mongolia: 67, Greenland + Svalbard + Scandes: 11, Canada: 6, Russia: 57, USA: 207), with overall 1835 match-up pairs in time.

Version 2 ALT Match up collection (1997 to 2018) (Validation in phase 2, CRDPv1 2020)

standardised annual ALT time series from 1997 and 2018 with a circum-Arctic geographic coverage. The collection was updated with ALT measurements from the GTN-P CALM program and contains data from 156 sites with 1835 match-up pairs.

Please note that we excluded all sites in Mongolia, Central Asia, and on the Tibetan Plateau (China). Please also note that we excluded in the 2020 validation also all sites within the Siberian Yedoma area (Bryant et al., 2017) due to incorrect parameterisation of Permafrost_cci CryoGrid of the Yedoma stratigraphy.

Version 3 ALT Match up collection (1997 to 2019) (Validation in phase 3, CRDPv2 2021)

standardised annual ALT time series from 1997 and 2018 with a circum-Arctic geographic coverage. The collection was updated with ALT measurements from the GTN-P CALM program, included the Yedoma regions and therefore, contains considerably more data, from 314 sites. Please note that we still excluded all sites in Mongolia, Central Asia, and China.

2.3.2 Characteristics of ALT Match-up Data Set

The ALT match up v3 data set (2021) contains standardized in situ ALT matched with *CRDPv2* Permafrost_cci ALT. Figure 2.9 shows the frequency distribution of the match-up data. In situ ALT can, by definition, only occur within permafrost. Therefore, the characteristics of the ALT Permafrost_cci and ALT in situ data collections represent all data sampled in permafrost zones.

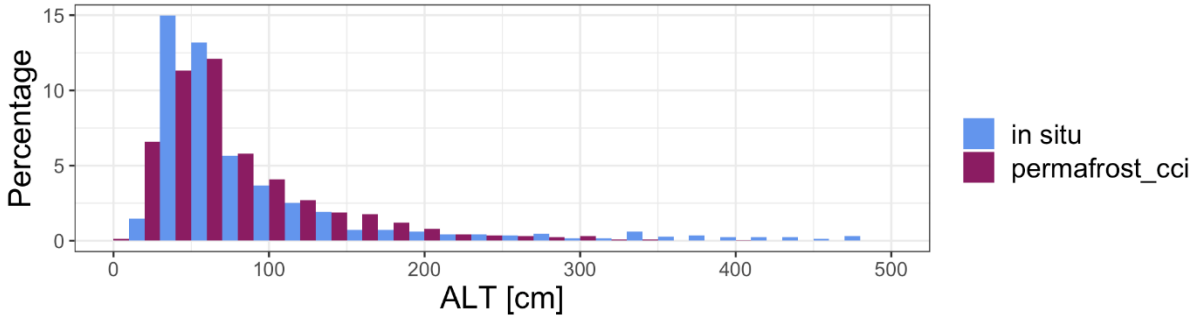

Figure 2.9: Frequency distribution of Permafrost_cci ALT and in situ ALT from GTN-P CALM.

The characteristics of Permafrost_cci ALT show an unimodal right-skewed distribution with a maximum around 40 to 80 cm ALT (Figure 2.9). Both Permafrost_cci ALT and in situ ALT show highest abundance in shallow ALT values with the most abundant in situ ALT data in the depth range of 40 to 60 cm.

2.4 Assessment of Permafrost Extent

2.4.1 Permafrost Fraction Reference Data

In Perrmafrost_cci we approximate permafrost abundance with the GTD and ALT reference data sets.

Within the first validation round of Permafrost_cci CRDPv0 PFR we applied a binary match-up assessment. We allowed a small variability around MAGT 0 °C not setting "permafrost" strictly as in situ MAGT <0 °C in 2 consecutive years. This approach in [RD-7] was successful and we applied it more in depth for the assessments of Permafrost_cci CRDPv1 and CRDPv2 PFR adding the ALT time series.

Match-up Version 1 Permafrost Fraction PFR, 2003 to 2017 (CRDPv0 2019)

- Permafrost_cci PFR per site and year in 0, 20, 40, 60, 80 or 100% Permafrost
- Binary PFR data set compiled from GTDv1: Permafrost abundance:
- Yes if all measurements in depths (0 – 2m) MAGT ≤0.5 °C.
- Criteria permafrost abundance yes / no

Match-up Version 2 Permafrost Fraction PFR, 1997 to 2018 (CRDPv1 2020)

- Permafrost_cci PFR per site and year in 0, 14, 29, 43, 57, 71 or 100% Permafrost
- Binary PFR data set compiled from GTDv2, ALTv2
- ALD from Russian expeditions (Bartsch, oral communication, 2020)
- Yes if any measurements in depths (0 – 2.4 m) MAGT ≤0.5 °C and Yes to all ALT <300 cm
- Criteria permafrost abundance yes / n

Match-up Version 3 Permafrost Fraction PFR, 1997 to 2019 (CRDPv1 2021)

- Permafrost_cci PFR per site and year in 0, 14, 29, 43, 57, 71 or 100% Permafrost
- Binary PFR data set compiled from GTDv3, ALTv3
- ALD from Russian expeditions (Bartsch, oral communication, 2020)
- Yes if any measurements in depths (0 – 2.4 m) MAGT ≤0.5 °C and Yes to all ALT <300 cm
- Criteria permafrost abundance yes / n

2.4.3 PERMOS Reference PFR Data Generation

The best visual expression of mountain permafrost is represented by rock glaciers, which, in contrast to the sub-ground permafrost itself, can be mapped and monitored directly using remotely sensed data. Rock glaciers are lava stream-like mixtures of permanently frozen debris that creep downslope under gravity. Their abundance can be used as validation for the high permafrost probability extent.
The information on rock glacier abundance and extent was computed within the GlobPermafrost program and is available since 2017 for the Bas-Valais region (Figure 2.10). From this inventory, PERMOS specifically selected the landforms indicative for permafrost occurrence (i.e., rock glaciers, push-moraines and complex landforms including both rock glaciers and push-moraines) and compared their occurrence with the Permafrost_cci PFR product.

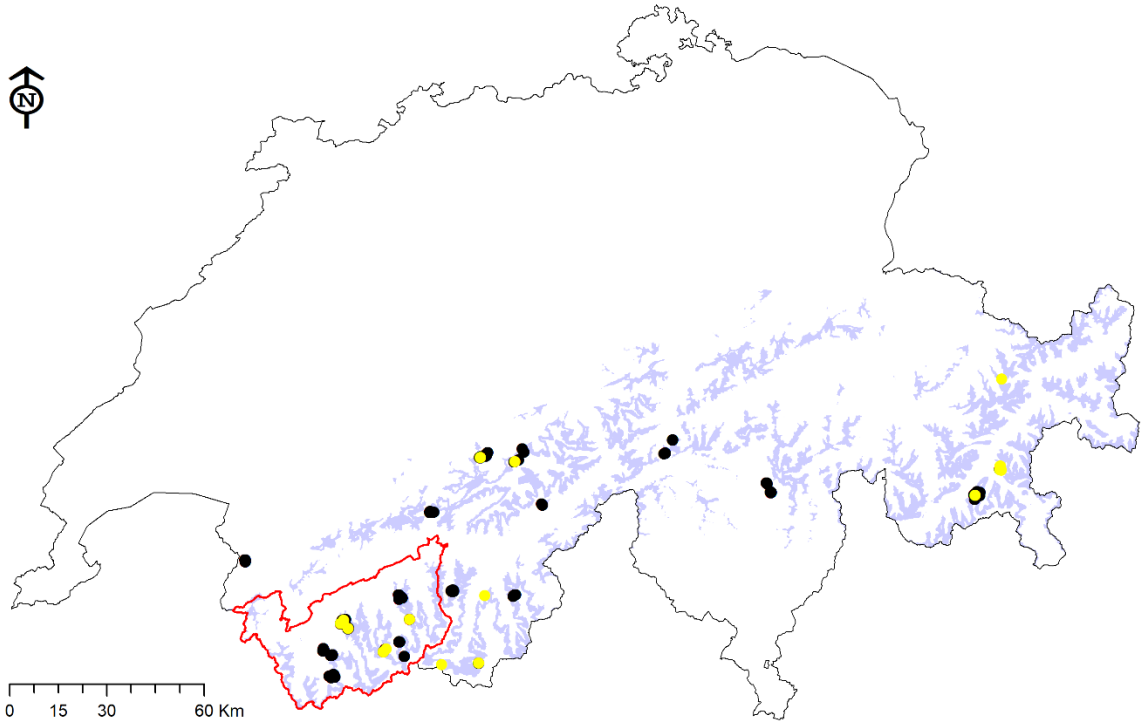

Figure 2.10. Location of the 247 GST logger (black circles), 27 GT boreholes (yellow circles) and the extent of the ESA GlobPermafrost rock glacier inventory (red outline) used for the validation of the Permafrost_cci GTD and Permafrost_cci PFR products in the Swiss Alps. The bluish colour-coded zones represent the areas located between 2500 m and 3000 m a.s.l.

3 ASSESSMENT RESULTS: PERMAFROST TEMPERATURE

3.1 Permafrost Temperature User Requirements

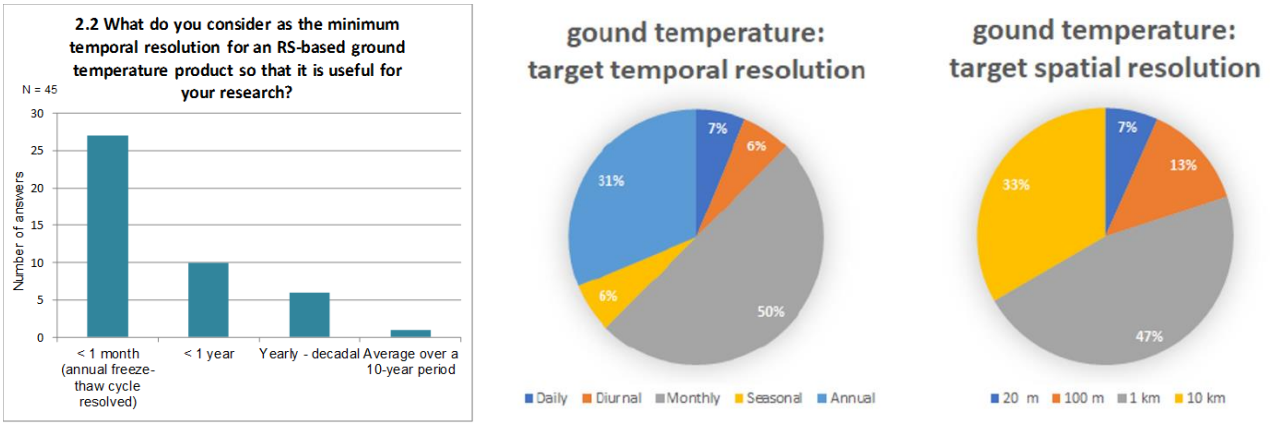

Figure 3.1a,b. User Survey results. Left: ESA DUE GlobPermafrost User Survey results, question 2.2 [RD-1]. Right: ESA CCI Permafrost User Survey results, Figure 3 [RD-4].

Users of potential products of permafrost temperature are interested in high temporal resolution: monthly or higher as documented in [RD-1, RD-2, RD-4]. However, 30% of users also rated annual resolution as adequate as target temporal resolution in [RD-4]. Half of the user group are satisfied with a target spatial resolution of 1 km. The first release of the Permafrost_cci CRDPv0 MAGT provided annual resolution with 1×1 km spatial resolution over a range of depths (0, 1, 2, 5, 10 m) from 2003 to 2017, the 2nd and 3rd release Permafrost_cci CRDP MAGT provides annual resolution with 1×1 km resolution over the same range of depths (0, 1, 2, 5, 10 m) but covering a longer time span from 1997 to 2018 and from 1997 to 2019.

3.2 Permafrost_cci MAGT Match-up Analyses with In Situ Data

The match-up was performed for Permafrost_cci MAGT versus in situ MAGT and a focus on the entire MAGT data collection as well as on a subset of measurements from permafrost temperatures only (in situ MAGT <1 °C). For each in situ point location and year, the pixel value in the Permafrost_cci products closest to the in situ measurement was extracted to compile the match-up data set and calculate summary statistics.

For further in depth analyses, we extracted the residuals of the match-up pairs from the 1:1 line and ran summary statistics on the entire dataset as well as the temperature related subsets. Furthermore, we used spatial visualisations to illustrate potential geographic biases in residuals.

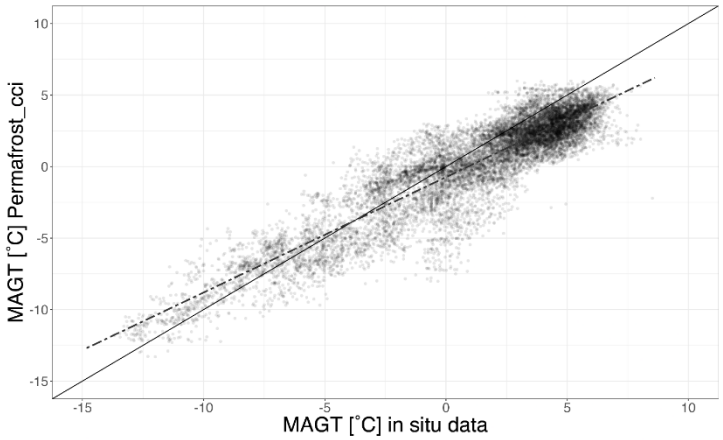

	all	< 1°C	≥ 1°C
bias	-0.98	-0.01	-1.46
abs_bias	1.58	1.46	1.63
RSME	1.93	1.87	1.97
slope	0.80	0.84	-0.58
intercept	-0.73	-0.54	0.75

Figure 3.2. Regression of Permafrost_cci MAGT versus in situ MAGT in all discrete depths and across all years. Summary statistics of Permafrost_cci MAGT versus in situ MAGT in all discrete depths are given for the entire dataset and the temperature related subsets.

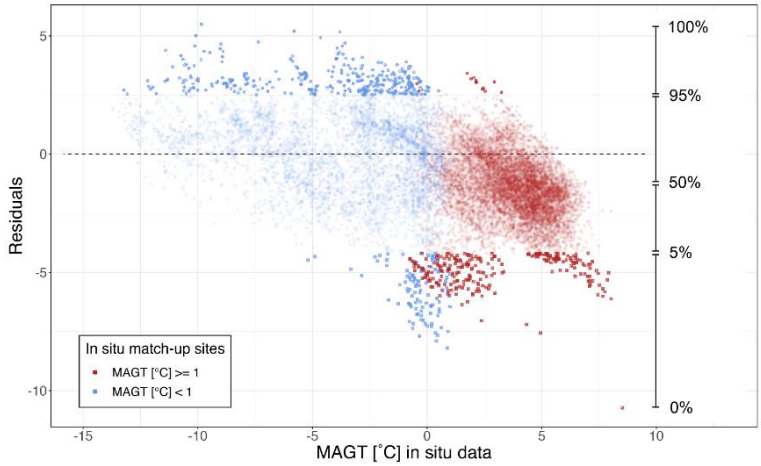

	all	< 1°C	≥ 1°C
100%	5.49	5.49	3.41
95%	2.51	3.18	1.13
50%	-1.12	0.20	-1.47
5%	-4.19	-4.09	-4.20
0%	-10.73	-8.21	-10.73

Figure 3.2. Residuals of Permafrost_cci MAGT SIN and in situ MAGT match-up with summary statistics for the entire dataset and the temperature related subsets.

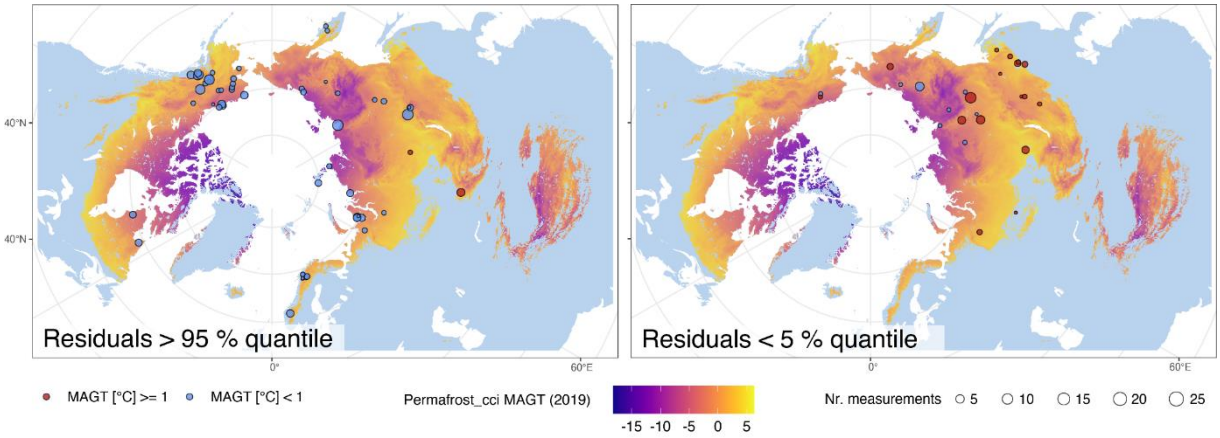

Figure 3.3 Location of residuals > 95% quantile (left) and < 5% quantile (right). Color of circles represents the temperature subset and size of the circle represents the number of samples at the particular location.

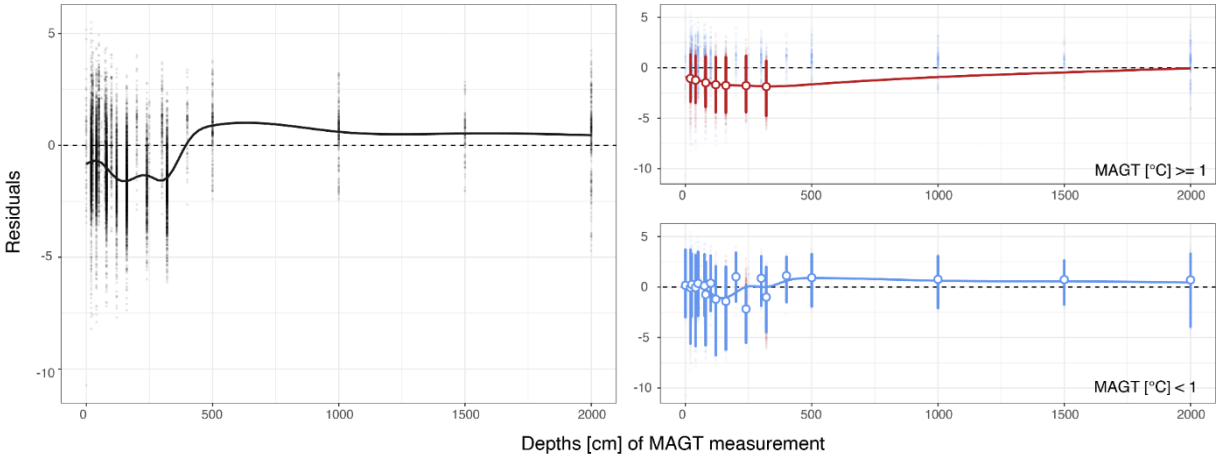

Figure 3.4 MAGT match-up residuals over sampling depths for the entire dataset (left) and the temperature related subsets (MAGT >=1°C; topright, MAGT <1°C; bottomright). The straight lines provide the median prediction of a generalised additive model (gam(Residual~s(Depth))). The error bars indicate the median and the 95% quantile of the residuals at a certain depth (n_depth = 50).

Table 3.1: Summary statistics of MAGT match-up residuals over sampling depths and temperature subsets.

	Complete Match-up						MAGT < 1°C						MAGT >= 1°C					
Depth [cm]	N	Min	5%	Median	95%	Max	N	Min	5%	Median	95%	Max	N	Min	5%	Median	95%	Max
0	76	-10.73	-3.22	**0.10**	3.57	5.17	72	-3.45	-2.99	**0.17**	3.71	5.17	4	-10.73				1.05
20	2,052	-8.21	-3.81	**-0.96**	2.03	5.49	409	-8.21	-5.58	**-0.05**	3.70	5.49	1,643	-7.05	-3.34	**-1.06**	1.30	3.18
25	470	-7.57	-2.94	**0.16**	3.24	4.66	441	-3.63	-2.89	**0.25**	3.29	4.66	29	-7.57				1.70
40	2,018	-7.90	-3.74	**-1.09**	1.81	4.34	388	-7.90	-5.84	**-0.04**	3.15	4.34	1,630	-7.20	-3.46	**-1.22**	1.16	2.66
50	488	-3.57	-2.93	**0.26**	3.48	4.92	460	-3.57	-2.82	**0.37**	3.48	4.92	28	-2.98				1.84
60	19	-2.70				3.09	19	-2.70				3.09						
75	348	-3.73	-2.82	**0.11**	3.23	4.29	338	-3.73	-2.83	**0.13**	3.24	4.29	10	-1.43				1.82
80	1,976	-7.19	-4.07	**-1.43**	1.48	4.34	352	-7.19	-5.75	**-0.74**	2.51	4.34	1,624	-6.37	-3.87	**-1.48**	1.08	3.05
100	252	-3.85	-2.63	**0.36**	3.06	4.05	237	-3.85	-2.36	**0.39**	3.11	4.05	15	-2.74				1.71
120	1,075	-7.69	-4.87	**-1.57**	1.41	3.41	177	-7.69	-6.75	**-1.20**	2.04	2.71	898	-5.98	-4.39	**-1.68**	1.04	3.41
160	1,939	-7.38	-4.52	**-1.72**	1.22	3.12	271	-7.38	-6.20	**-1.42**	2.01	2.62	1,668	-5.97	-4.43	**-1.75**	1.04	3.12
200	109	-2.88	-1.70	**0.99**	3.40	4.02	106	-2.88	-1.42	**1.03**	3.40	4.02	3	-2.66				-0.16
240	715	-5.99	-4.55	**-1.79**	1.12	2.79	51	-5.99	-5.52	**-2.17**	0.11	0.28	664	-5.44	-4.39	**-1.76**	1.18	2.79
250	31	-1.92				1.96	31	-1.92				1.96						
300	210	-3.07	-1.85	**0.87**	3.04	3.70	209	-3.07	-1.85	**0.87**	3.04	3.70	1	-1.36				-1.36
320	1,333	-6.12	-4.74	**-1.80**	0.97	2.36	130	-5.21	-4.47	**-1.00**	1.99	2.36	1,203	-6.12	-4.75	**-1.87**	0.65	1.94
400	88	-2.65	-1.48	**1.11**	2.97	3.36	86	-2.65	-1.50	**1.13**	3.00	3.36	2	-0.30				0.32
500	225	-2.40	-1.92	**0.90**	3.25	3.76	220	-2.40	-1.92	**0.93**	3.25	3.76	5	-1.40				-0.71
1000	234	-2.43	-2.07	**0.76**	3.04	3.22	230	-2.43	-2.07	**0.76**	3.04	3.22	4	-0.93				-0.89
1500	98	-2.04	-1.69	**0.64**	2.61	2.83	94	-2.04	-1.74	**0.74**	2.62	2.83	4	-0.56				-0.39
2000	351	-4.71	-3.92	**0.71**	3.29	4.22	351	-4.71	-3.92	**0.71**	3.29	4.22						
Summary	**14,107**	**-10.70**	**-4.19**	**-1.12**	**2.51**	**5.49**	**4,672**	**-8.21**	**-4.09**	**0.20**	**3.18**	**5.49**	**9,435**	**-10.70**	**-4.20**	**-1.47**	**1.13**	**3.41**

Permafrost_cci and in-situ MAGT consensus in temporal trends

We assessed the consensus in temporal trends between the MAGT in-situ and Permafrost_cci simulation by extracting the slope coefficient of a linear correlation of MAGT over years, separately for each site and depth and for in-situ and cci time series. Next, we calculated the difference between the in-site and the Permafrost_cci slope (Slope_in-situ - Slope_cci) and grouped the value into three different categories:

- Stable slope indicates that either both trends showed no significant change or both trends were significant and in the same direction (positive/negative).
- No trend to significant trend (or vice versa) indicates a change in significant level ($p<0.05$) but no change in direction.
- Positive to negative significant trend indicates a switch between the significant trend direction.

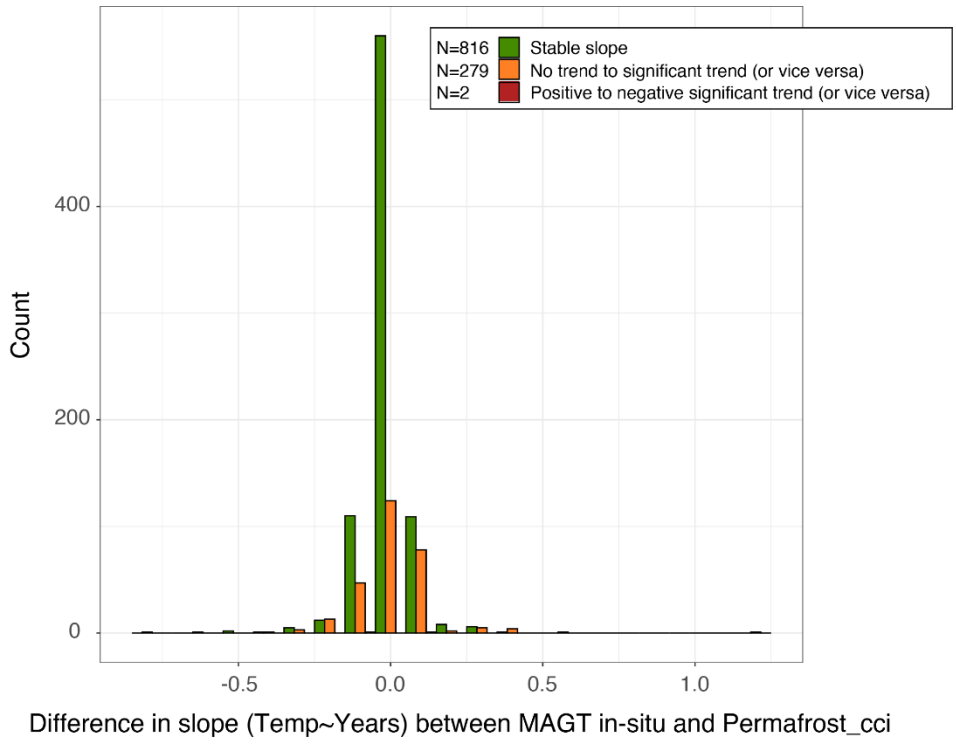

Figure 3.5: Frequency distribution of slope differences between the MAGT (in-site vs. cci) over time, grouped by the overall change characteristics.

Summary of MAGT match-up comparison across all years, temperature, and measuring depths (n = 14,107).

Permafrost Mean Annual Ground Temperature (MAGT) match-up evaluation between simulated Permafrost_cci and in situ measurements showed the following performance characteristics:

- Overall, the simulation dataset had a median MAGT bias of -1.12 °C (95% CI: -4.19 to 2.51 °C).

- Match-up pairs from in-site measurements with MAGT < 1°C and thus from reliable permafrost sites showed a better performance (**median bias of 0.2°C, 95% CI: -4.09 to 3.18 °C**), compared to the full dataset and notably in comparison to warmer sites with MAGT >= 1°C (median bias of-1.47, 95% CI: -4.20 to 1.13°C).
- Extreme residuals showed no obvious spatial clusters. However, a relatively large proportion of residuals >95% quantile were located across Alaska.
- Residuals across depths were rather stable with slightly larger negative median biases in lower depths (0-3m), mainly caused by negative biases in match-up pairs of warmer sites (MAGT >= 1°C).
- The trends in MAGT over years generally match between the in-situ measurements and the Permafrost_cci product (75%). In some cases (24%) the trends change from a significant trend (p>0.05) to no trend or vice versa. However, the range of differences in slopes within this group remains low (0.001, 95% CI: -0.22 to 0.29).

Permafrost Mean Annual Ground Temperature (MAGT) match-up evaluation between simulated Permafrost_cci and in situ measurements showed the following performance characteristics:

- Overall, the simulation dataset had a median MAGT bias of -1.12 °C (95% CI: -4.19 to 2.51 °C).
- Match-up pairs from in-site measurements with MAGT < 1°C and thus from reliable permafrost sites showed a better performance (median bias of 0.2°C, 95% CI: -4.09 to 3.18 °C), compared to the full dataset and notably in comparison to warmer sites with MAGT >= 1°C (median bias of-1.47, 95% CI: -4.20 to 1.13°C).
- Extreme residuals showed no obvious spatial clusters. However, a relatively large proportion of residuals >95% quantile were located across Alaska.
- Residuals across depths were rather stable with slightly larger negative median biases in lower depths (0-3m) mainly caused by negative biases in match-up pairs of warmer sites (MAGT >= 1°C).

3.3 PERMOS Permafrost Temperature

The comparison of the evolution of the mean in situ measured and modelled MAGST over the Swiss Alps from 1997 to 2019 shows that the model has a warm bias of +1.22 °C compared to the measurements. However, the warming tendency observed in the measurements is well reproduced by Permafrost_cci GTD product (Figure 3.6) as well as the inter-annual variation. The standard deviation of the in situ measurements, although limited to 23 sites, is larger than the standard deviation of the Permafrost_cci GTD product at 0 m over the entire Swiss Alps between 2500 and 3000 m a.s.l. This is emphasized in Figure 3.7 which shows the measured MAGST for each single logger in the PERMOS network compared to the minimum and maximum Permafrost_cci MAGT at 0 m depth modelled in-between 2500 and 3000 m a.s.l. in the Swiss Alps. The measured in situ data ranges from around -4 °C to +7.5 °C, whereas Permafrost_cci MAGT ranges from around -1 °C to +4.5 °C. Only few loggers exhibit MAGST values greater than the modelled range, whereas many have lower MAGST.

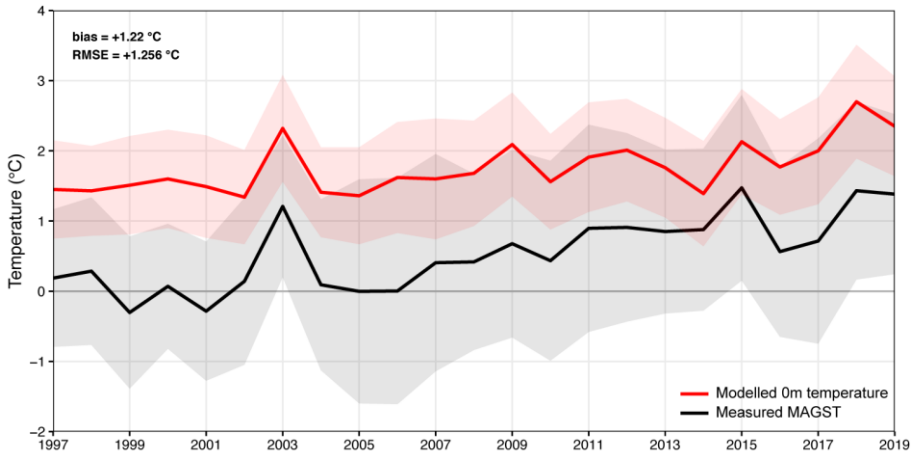

Figure 3.6. Temporal evolution of measured mean MAGST (black) and mean Permafrost_cci GTD at 0 m depth (red) over the entire Swiss Alps between 2500 and 3000 m a.s.l. The shaded area represent ± one standard deviation.

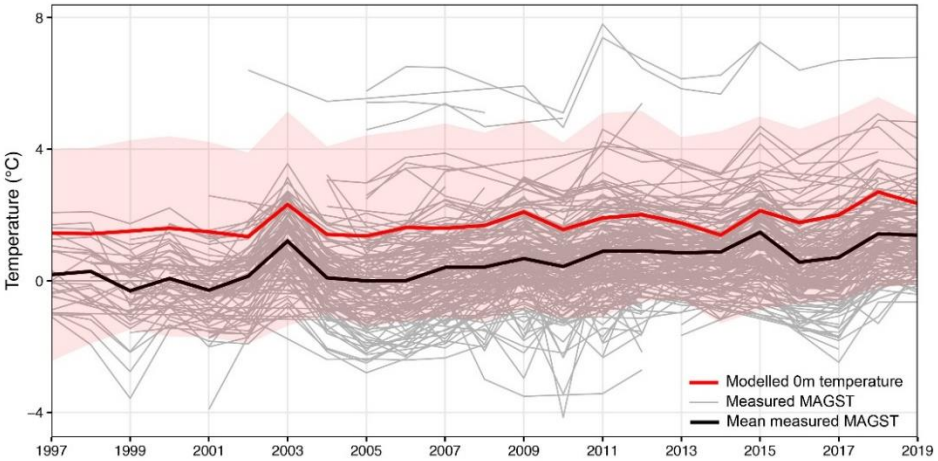

Figure 3.7. Temporal evolution of measured MAGST at all loggers in the Swiss Alps between 2500 and 3000 m a.s.l. (grey) compared to mean simulated Permafrost_cci GTD at 0 m depth (red). The shaded area represents the minimum and maximum GTD. The mean of all in situ measured sites is indicated in black.

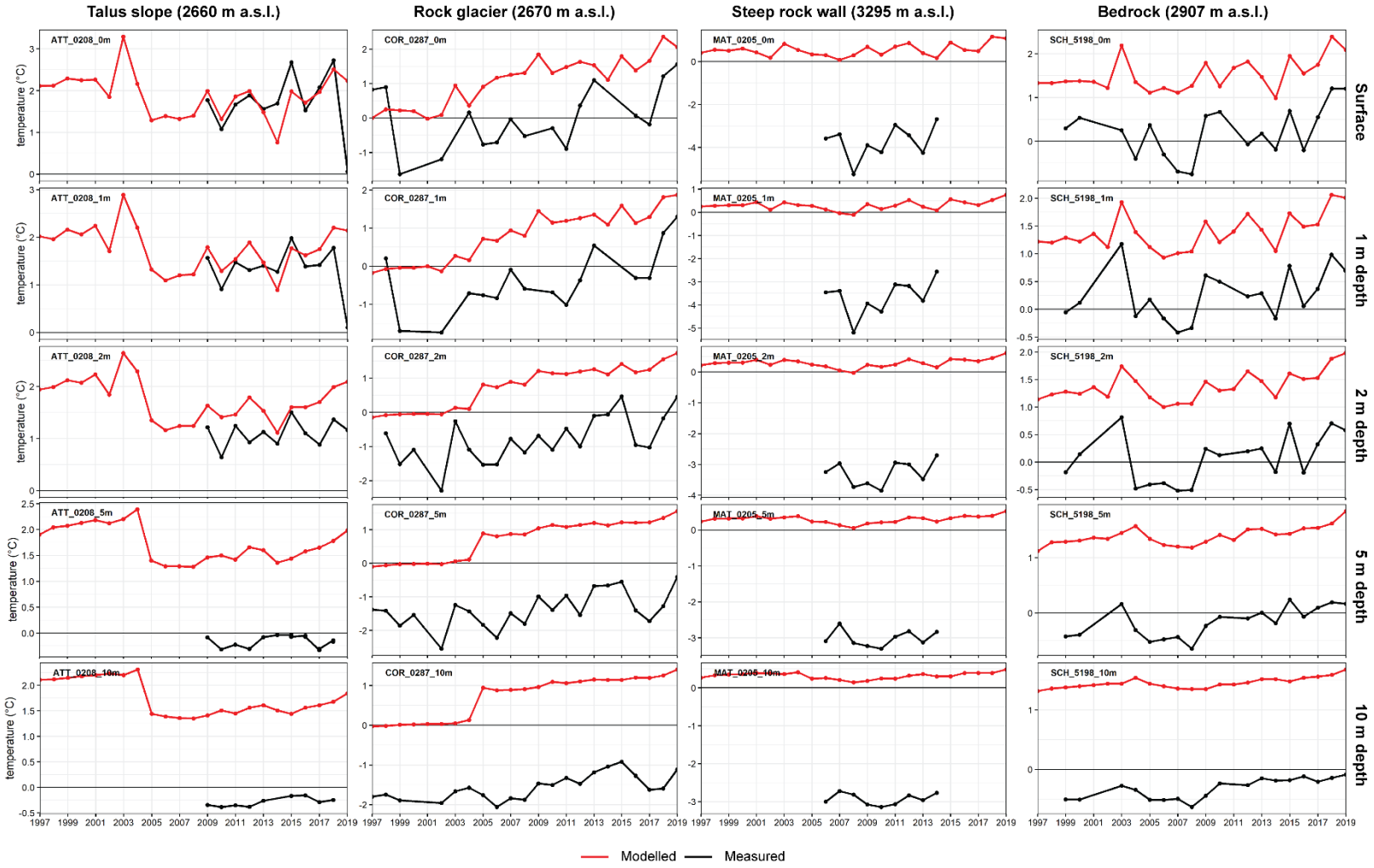

Figure 3.8. Comparison of simulated mean Permafrost_cci GTD (red) and in situ measured (black) MAGT at 0, 1, 2, 5 and 10 m depth at 4 sites in the Swiss Alps.

Comparing the modelled Permafrost_cci GTD at 0, 1, 2, 5 and 10 m depth to the in situ measured MAGT in boreholes (see Figure 3.7), Permafrost_cci GTD are systematically too warm at all depth and locations. The simulated Permafrost_cci GTD values fit better the in situ observations near the surface and the warm model bias increases with depth (+1.66 °C at 0 m and + 1.81 °C at 10 m, see Figure 3.21). The same pattern is found at all sites (Figure 3.8).

Although the absolute values are significantly different, both, the measured and the simulated MAGT, show a warming trend over the period 1997-2019. At depth, measured MAGT in 2017 show a more or less marked cooling effect. This is due to the extremely snow-poor winter 2016/17 in the Swiss Alps, which enabled the cold winter air temperature to cool more efficiently the ground (PERMOS 2019). This effect is not reproduced in Permafrost_cci simulations, illustrating the difficulty to include snow effects in global models.

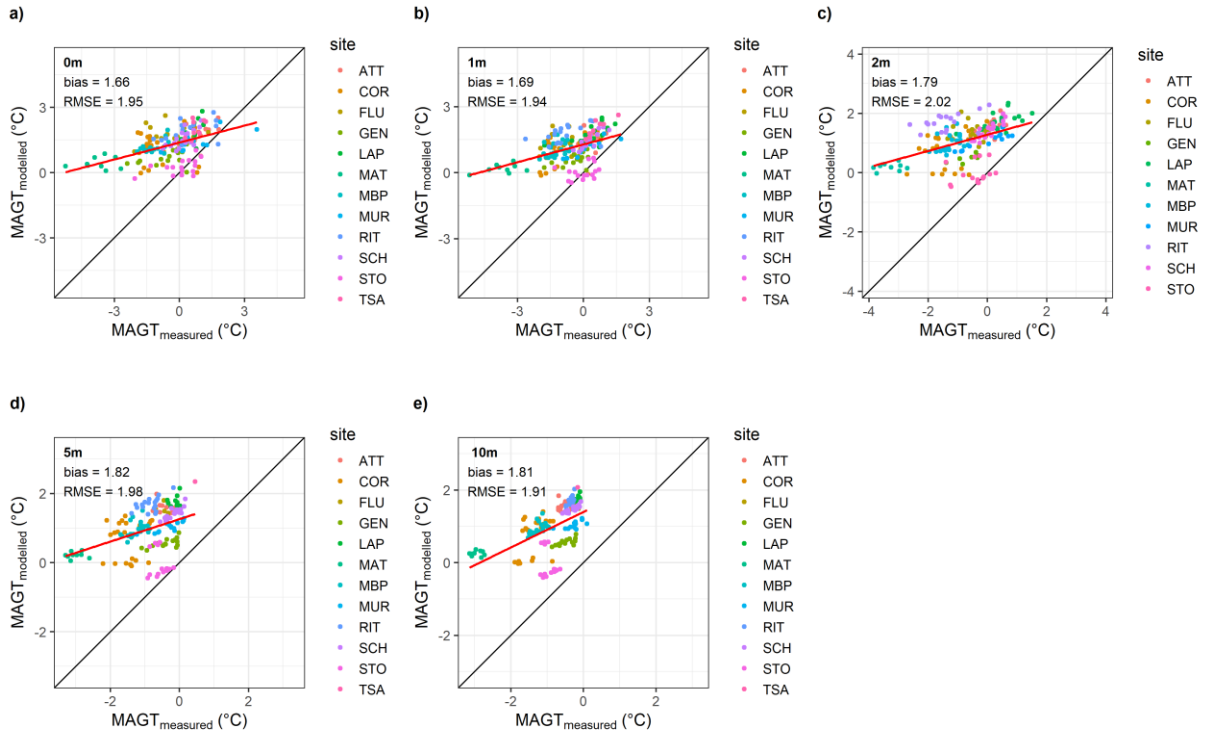

Figure 3.9. Comparison of simulated mean Permafrost_cci MAGT (y-axis) and in situ measured (x-axis). The black line represents the one-to-one relationship and the red one the best linear fit. Statistics are displayed for each depth.

3.4 Permafrost_cci MAGT Comparison vs FT2T MAGT

A comparison of Permafrost_cci MAGT POL at 0 and 2 m depth with FT2T derived ground temperatures for selected locations demonstrate the expected higher variability of surface state from year to year, but also agreement of the different data sources regarding temperature level (Figures 3.22 & 3.23). Deviations can be found for sites in the transition zone (temperatures around 0°C) in Alaska as well as Russia. FT2T results are closer to in situ records than CRDPv1 at Svetlyy in Central Siberia and Boza Creek, Alaska (Figures 3.24and 3.25). Specifically, Svetlyy is an outlier location regarding permafrost extent evaluation. Results of CRDPv1 for Nadym, Western Siberia agree better with in situ then FT2T results. FT2T is too cold at this location. Here, the covered ASCAT footprint (appr. 12.5 km) contains a wide range of vegetation types (tundra shrubs to tall floodplain shrubs) and comparably wet soils. Either the Nadym borehole site is not representative for the footprint (but is for the 1km CRDv1 grid) or soil type/snow cover play an important role for heat transfer (insulation) which is not represented in the simple FT2T approach.

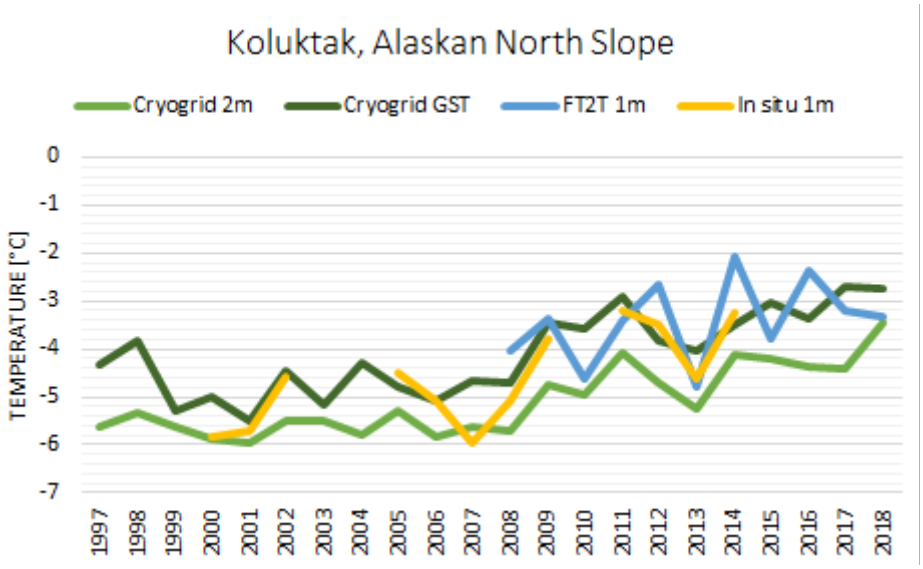

Figure 3.10. Comparison of FT2T product with CRDPv1 results and in situ data at Koluktak, Alaska.

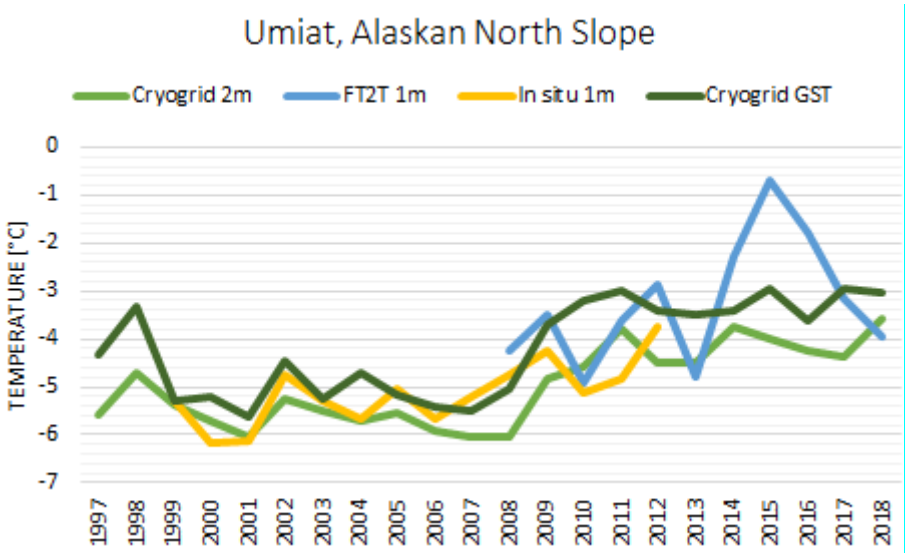

Figure 3.11. Comparison of FT2T product with CRDPv1 results and in situ data at Umiat, Alaska

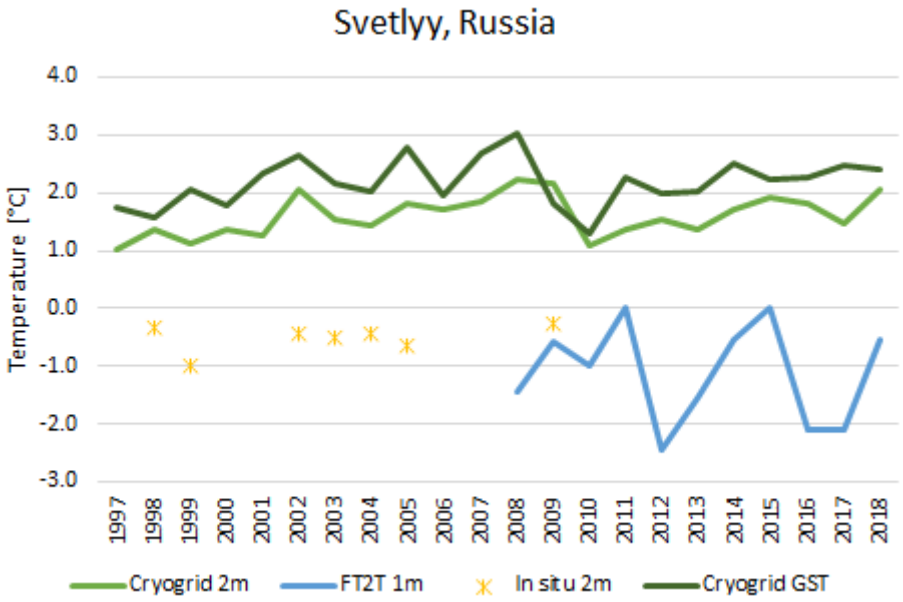

Figure 3.12. Comparison of FT2T product with CRDPv1 results and in situ data at Svetlyy, Central Siberia, Russia. See also permafrost extent discussion in section 5.1 and figure 5.6.

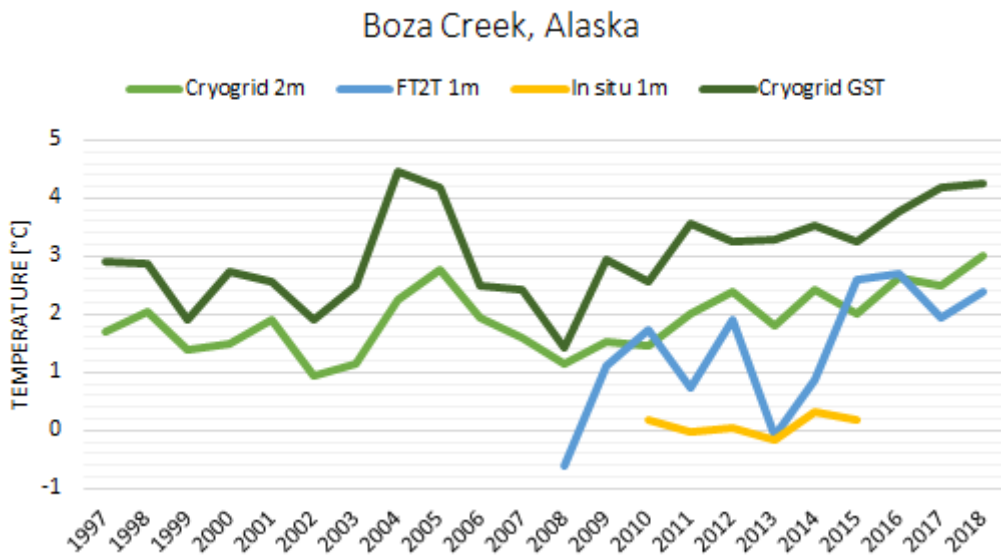

Figure 3.13. Comparison of FT2T product with CRDPv1 results and in situ data at Boza Creek, Alaska

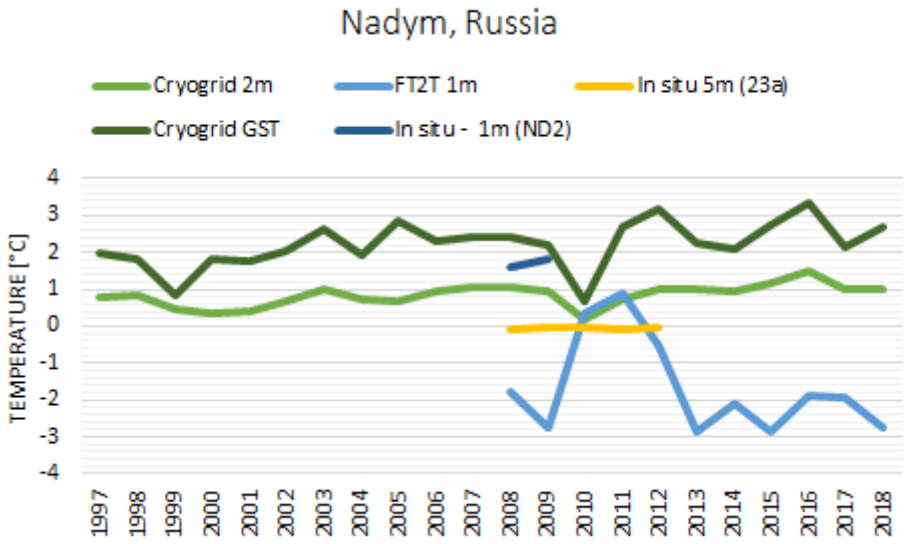

Figure 3.14. Comparison of FT2T product with CRDPv1 results and in situ data at Nadym, Western Siberia, Russia

Regional comparisons have been made for CRDPv2. This required the correction for water fraction as detailed in Bergstedt et al. (2020). The water class of Landcover_cci has been used to assign a water fraction for each original ASCAT footprint (hexagonal approximation as in Högström et al. 2018) overlapping with permafrost according to Permafrost_cci CRDPv2. The calibration of FT2T has been revised and extended to include 1m depth borehole data (North America) and 80cm depth data (Russian Arctic) in order to avoid a regional (and temperature range) bias. Regional aggregation of results was applied to countries and administrative districts.

Temperature averages partially correlate with R^2=0.45 (Alaska) and R^2=0.35 (Canada). No correlation can be observed for Russia and Greenland. An offset can be observed in case of Greenland and Alaska. This bias is similar for both regions and is about 1.5°C (Figure 3.15).

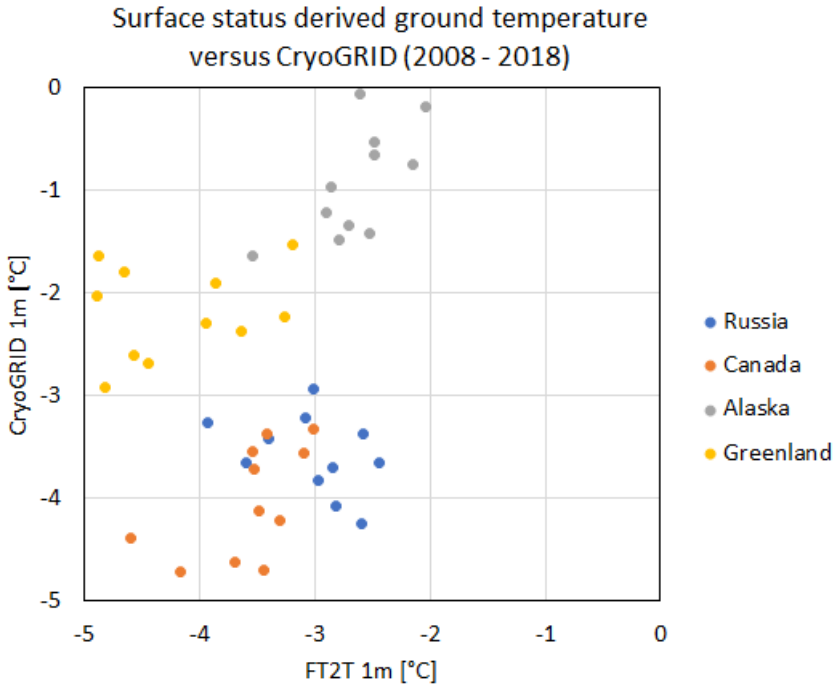

Figure 3.15: Regional average for areas with at least once <0°C. CRDPv2 versus Metop ASCAT derived ground temperature (from freeze/thaw - FT2T Model)

4 ASSESSMENT RESULTS: ACTIVE LAYER THICKNESS

4.1 Active Layer Thickness User Requirements

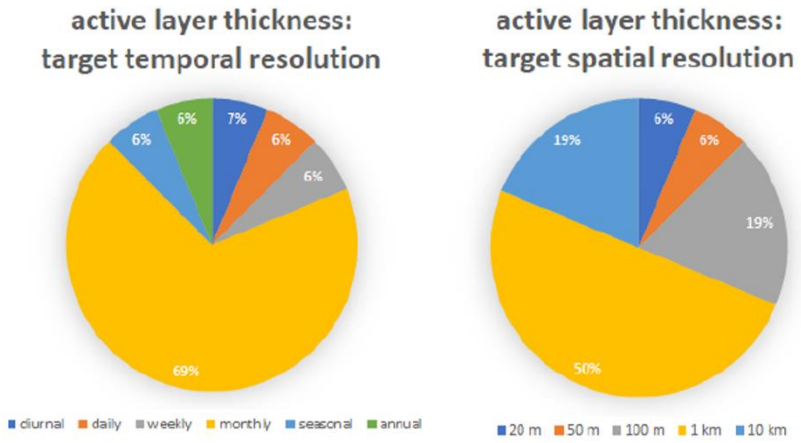

Figure 4.1. User Survey results. ESA CCI Permafrost User Survey results, Figure 4 [RD-4].

Users of potential products of active layer thickness are interested in high temporal resolution: monthly or higher in [RD-4]. Finally, less than 10% of users rated annual resolution as adequate as target temporal resolution in [RD-4]. However, the definition of the official ECV ALT is that it is the maximum thaw depth in summer and has by this the maximum temporal resolution of one year. Like this, the CRDP Permafrost_cci with ALT in annual resolution is the highest temporal resolution possible for this Permafrost ECV. Users were interested in higher temporal resolution, the representation of thaw depth that is developing deeper throughout the summer season until reaching the maximum depth in late summer, the ALT. But seasonal thaw depth evolution is not considered an ECV (see also glossary in section 1.7). Half of the user group are satisfied with a target spatial resolution of 1 km. The 1^{rst} release of the Permafrost_cci CRDPv0 ALT provided annual resolution with the required 1×1 km spatial resolution from 2003 to 2017. The 2nd and 3rd release of Permafrost_cci CRDP ALT provide annual resolution with the required 1×1 km² spatial resolution with a longer time span from 1997 to 2018 and in the latest version 3 until 2019.

4.2 Permafrost_cci ALT Match-up Analyses with In Situ Data

For each in situ point location, the pixel in Permafrost_cci ALT products closest to the in situ measurement was extracted to produce the match-up data set and derive comparisons and summary statistics. ote that we assessed the fitness of Permafrost_cci ALT with focus on the Northern Hemisphere high-latitude continuous permafrost region. The midlatitude discontinuous permafrost regions on high plateaus in Mongolia, Central Asia and China (e.g., Tibetan Plateau) are characterised by very different snow regimes and subground properties requiring further model parameterisation. We therefore excluded all sites in Mongolia, Central Asia, and on the Tibetan Plateau (China) to allow an adequate assessment of mid-latitude to high-latitude permafrost regions.

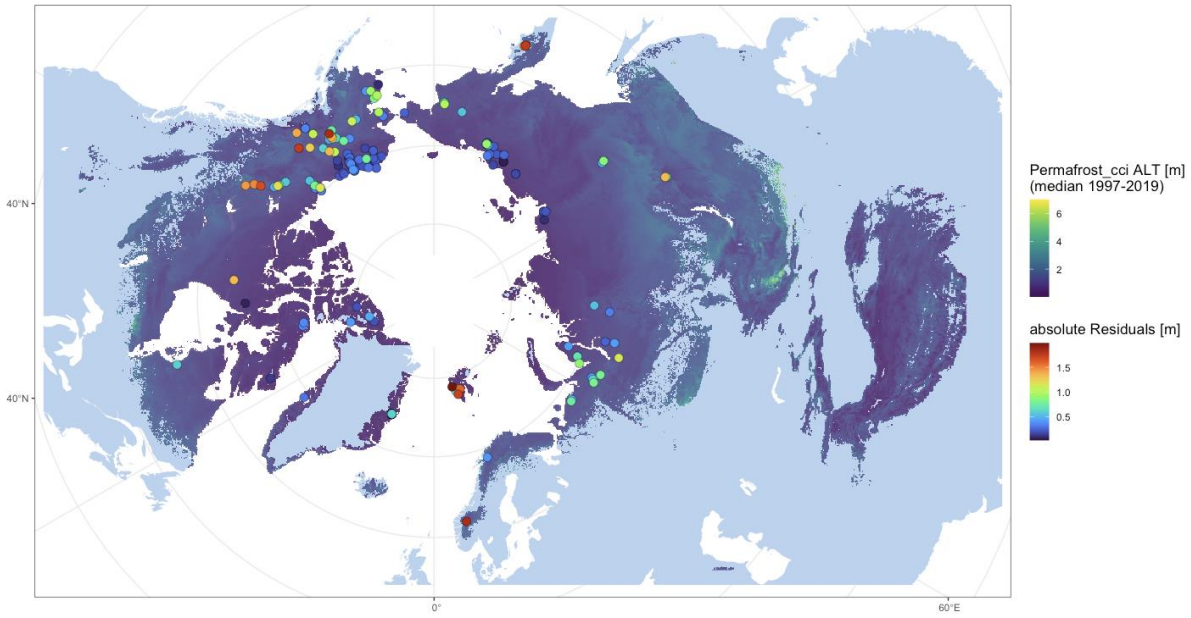

Figure 4.2. Spatial distribution of maximum residual per site from Permafrost_cci ALT and in situ ALT match-up over active layer thickness depths in cm.

Large residuals >1 m are obvious in the warmer permafrost zones in forested regions of Alaska, Canada and Central Siberia (Permafrost_cci negative bias with simulated shallow ALT versus deep in-situ ALT) (Figure 4.2). Also residuals >1.5 m cluster in Svalbard (Figure 4.2) (Permafrost_cci positive bias with simulated deep ALT versus shallow in-situ ALT).

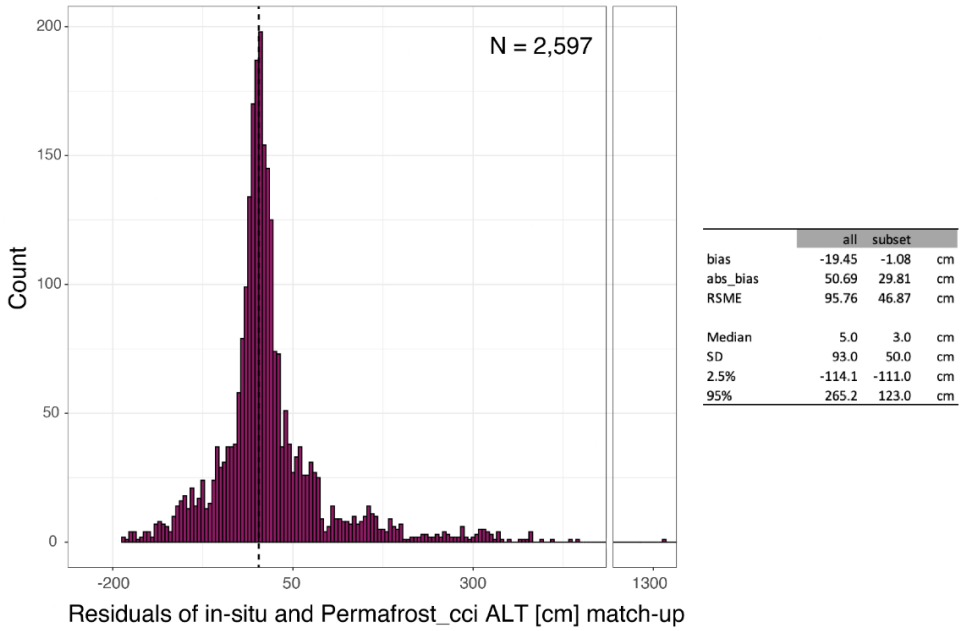

Figure 4.3. Frequency distribution of Permafrost_cci ALT minus in situ ALT. Summary statistics including all ALT Match-up data pairs and with locations from Mongolia, and China excluded (N_excluded = 314).

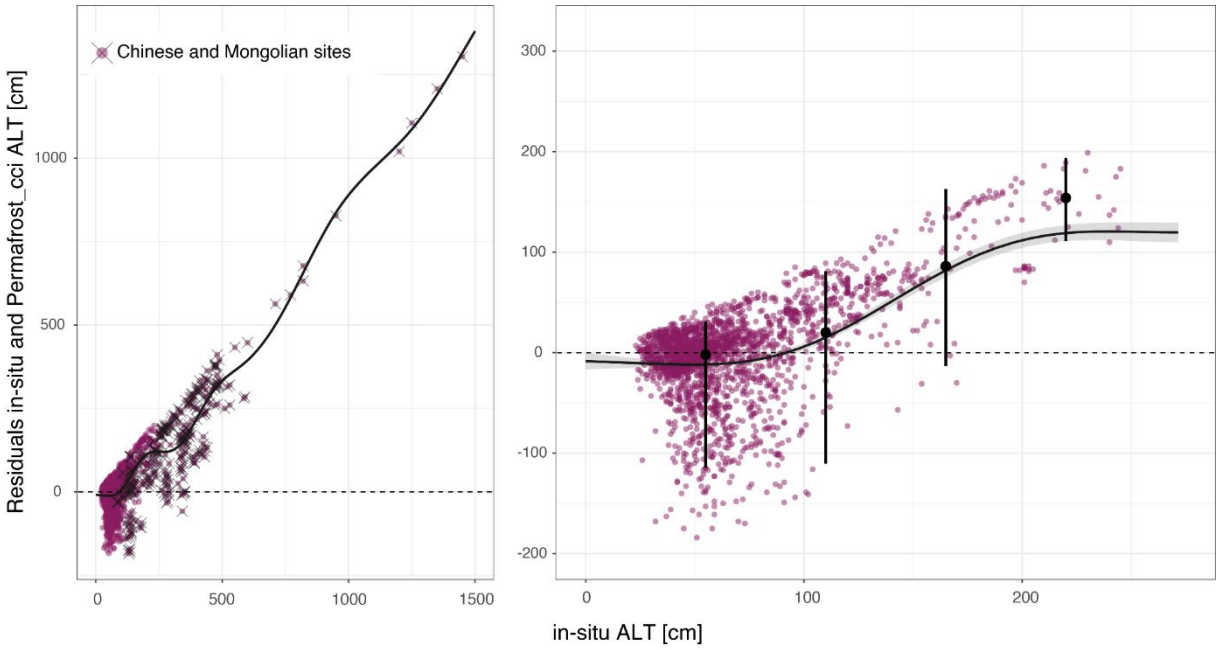

	Across all depths	0-55 cm	>55-110 cm	>110-165cm	>165-220cm
100%	-184.0	-184.0	-170.0	-57.0	110.0
95%	-111.0	-115.0	-111.0	-13.1	111.0
50%	**3.0**	**-2.0**	**20.0**	**86.0**	**154.0**
5%	123.0	31.0	81.0	163.0	194.0
0%	199.0	51.0	115.0	173.0	199.0

Chinese and Mongolian sites excluded

Figure 4.4. Residuals from Permafrost_cci ALT and in situ ALT match-up over active layer thickness depths in cm. Crossed out circles belong to in-situ sites located in China and Mongolia. These sites were excluded from further assessment (see details in text). Solid lines present median prediction values from a generalised additive model (gam(Residual~s(Depth)). Summary statistics are presented for all depths and for four bins that are also visualised as error bars in the right panel.

Permafrost_cci and in-situ ALT consensus in temporal trends

We assessed the consensus in temporal trends between the ALT in-situ and Permafrost_cci simulation by extracting the slope coefficient of a linear correlation of ALT over years, separately for each site and for in-situ and Permafrost_cci time series. Next, we calculated the difference between the in-situ and the Permafrost_cci slope (Slope_in-situ - Slope_cci) and grouped the value into three different categories:

- Stable slope indicates that either both trends showed no significant change or both trends were significant and in the same direction (positive/negative).
- No trend to significant trend (or vice versa) indicates a change in significant level ($p<0.05$) but no change in direction.
- Positive to negative significant trend indicates a switch between the significant trend direction.

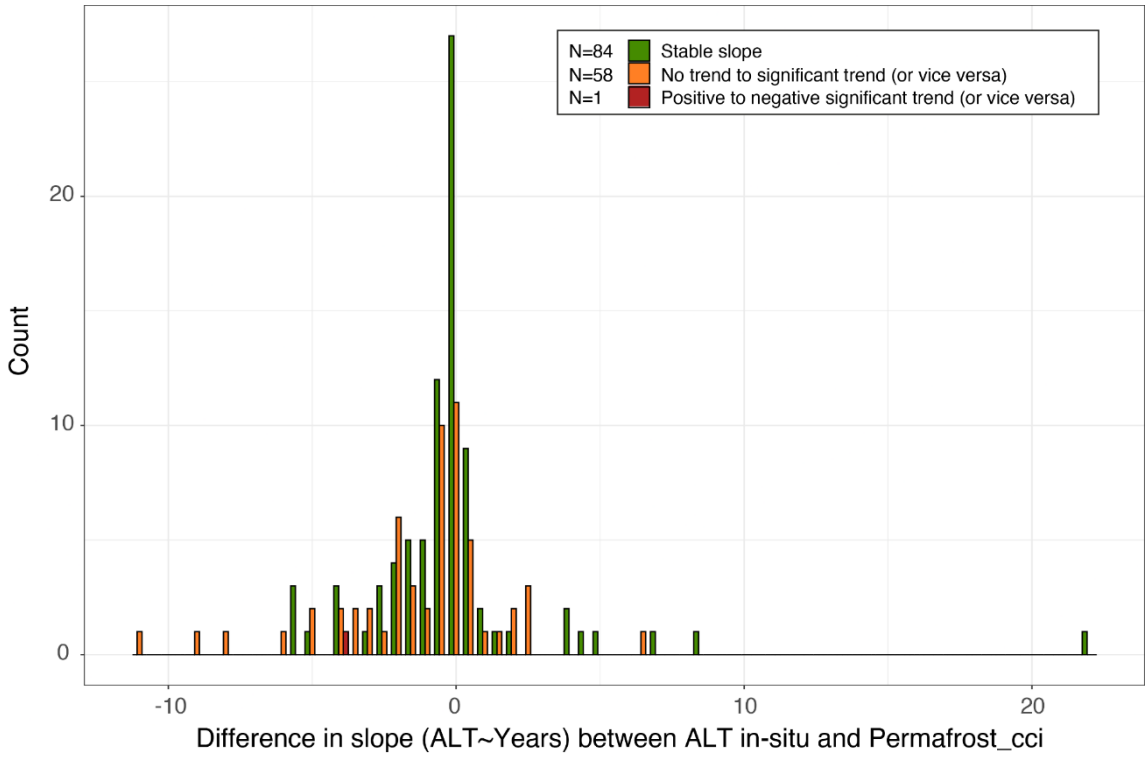

Figure 4.6: Frequency distribution of slope differences between the ALT (in-site vs. cci) over time, grouped by the overall change characteristics.

Summary of match-up comparison of in-situ and Permafrost_cci ALT time series collection (1997 to 2019; N = 2,283)

Permafrost_cci ALT performance for in situ ALT with match-up paris from China and Mongolia excluded is characterised by:

- a median bias of 3 cm (95% CI: -11 to 123 cm).
- bias is smallest in the shallow active layers with a median deviation of -2 cm (95% CI: -115 to 31 cm).
- Permafrost_cci residuals > 1 m (with Permafrost_cci shallow ALT versus deep in-situ ALT) in forested regions of Alaska, Canada and Siberia.
- Permafrost_cci residuals > 1.5 m in Svalbard (with Permafrost_cci deep ALT versus shallow in-situ ALT).
- differences in trends over time between Permafrost_cci and in-situ measurements are larger compared to the MAGT product (note ALT match-up sample size is also considerably smaller). The majority (58%) of Permafrost_cci ALT trends over time match the in-situ trends. Except for one match-up pair, the remaining trends (40%) differ and switch between no trend to significant trend or vice versa (95% interval of slope differences; -8.57 to 2.57).

5 ASSESSMENT RESULTS: PERMAFROST EXTENT

5.1 Permafrost_cci PFR Match-up Analyses with In Situ Data

The match-up dataset contains in-situ binary information on permafrost existence (FALSE/TRUE) and simulated yearly fraction of permafrost-underlain and permafrost-free area within a pixel (PFE) across four different percentage groups (14, 29, 43, 57, 71, 86, 100 %). Using both, ALT and MAGT in-situ measurements, the match-up data set contains n = 539 pairs/sites.

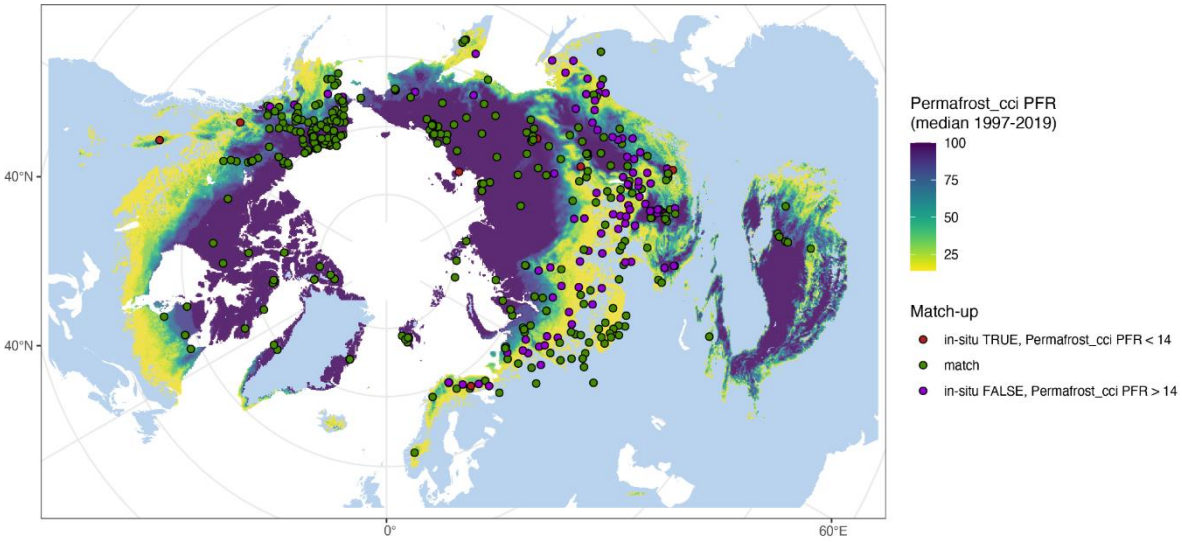

Figure 5.1: Spatial distribution of PFE match-up pairs grouped by matching characteristics. The underlying map shows the median Permafrost_cci permafrost extent product.

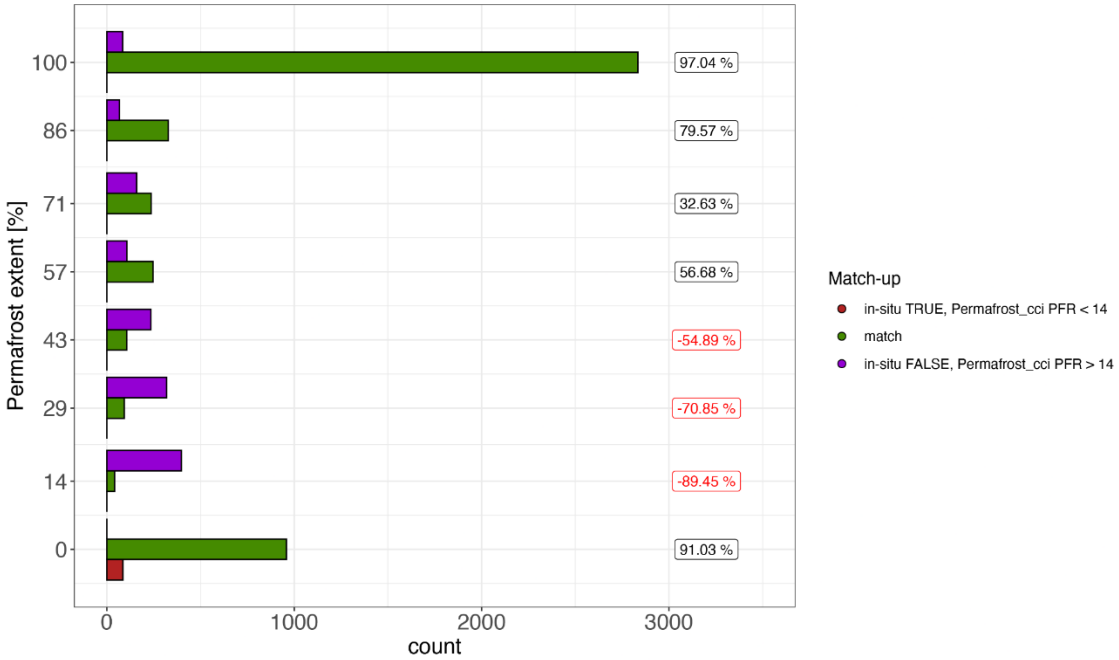

Figure 5.2: Match-up summary of Permafrost_cci PFR with in-situ MAGT and ALT dataset. The percentage values depict the accuracy of the match up across permafrost-underlain and permafrost-free area values within a pixel.

As a consequence of the cold bias in the warm temperature range, the binary match-up of 'permafrost' versus 'no permafrost' for Permafrost_cci PFR versus in situ MAGT ranges shows that PFR in the grid cell is overestimated compared to in situ-derived 'no permafrost' and MAGT ≤0.5 °C. Permafrost_cci PFR in the grid cell >0% occurs together with a wide range of 'warm' in situ MAGT >0 °C. Overall, the majority of match-up pairs (69.9%) were in agreement between the in-situ proxy and the Permafrost_cci simulation (Figure 5.2). Notably, the 100% and the 0% PFR had high percentage of agreement, with 97.04% and 91.03% match respectively.

Permafrost_cci and in-situ PFR temporal stability

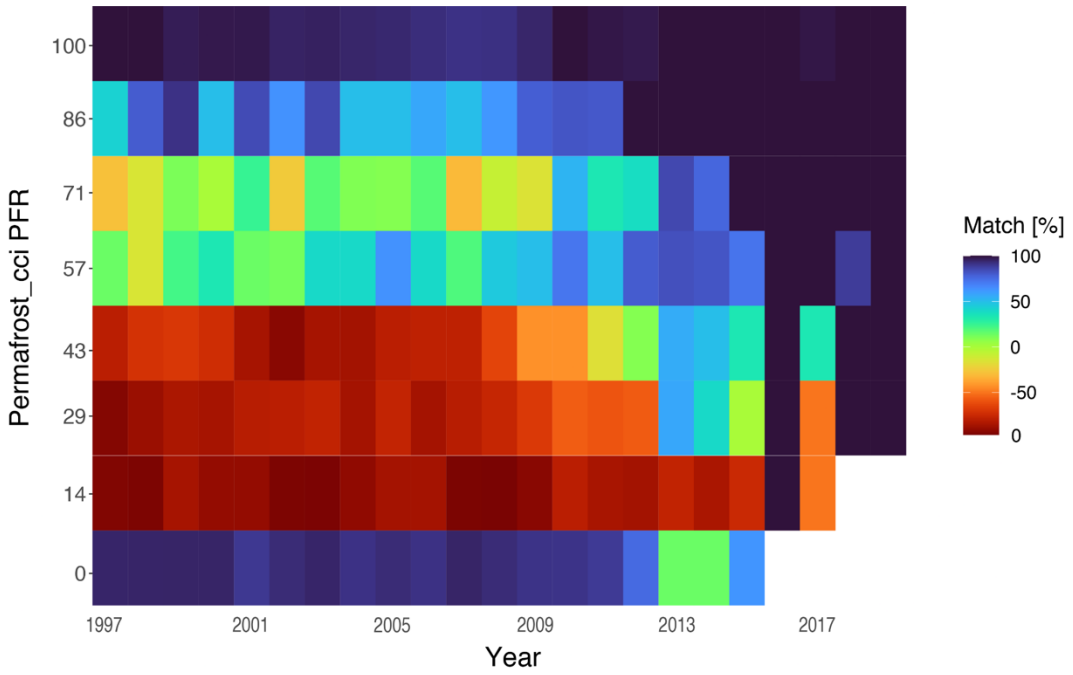

Figure 5.3: Match-up summary of Permafrost_cci PFR with in-situ MAGT and ALT dataset over years.

Summary of match-up comparison of in-situ proxies and simulated Permafrost_cci PFR (1997-2019: N = 539).

Permafrost_cci PFR performance measured against in-situ proxies is characterised by:

Overall, the majority of match-up pairs (69.9%) were in agreement between the in-situ proxy and the Permafrost_cci simulation.
Notably, the 100% and the 0% PFR had high percentage of agreement, with 97.04% and 91.03% match respectively.
Geographically, most mismatches were located in the Eurasian southern boundary of the permafrost extent.
The high agreement in the 100% and 0% Permafrost_cci PFR groups was stable across years. In general, the agreement in the <100% and >0% groups increased towards the end of the time series (2019).

5.2 PERMOS Permafrost Extent

Figure 5.4 compares the simulated Permafrost_cci PFR in 2019 in the Bas-Valais region with the slope movement inventory compiled for the same region within the ESA GlobPermafrost program (green polygons) and the location of the PERMOS boreholes (yellow dots). Within the GlobePermafrost inventory, we selected only the landforms classified as rock glaciers, push moraines or a complex combination of the two, since they are the ones representative of permafrost occurrence. The blue colour represents Permafrost_cci grid cells with PFR > 0% in 2019. One can clearly see that the extent of permafrost simulated by Permafrost_cci PFR (i.e. PFR >0%) is too restrictive. In the Swiss Alps, the lower limit of permafrost is usually found around 2600 m a.s.l. ± 200 m and within the simulated Permafrost_cci PFR the lower limit is found around 3000 m a.s.l..

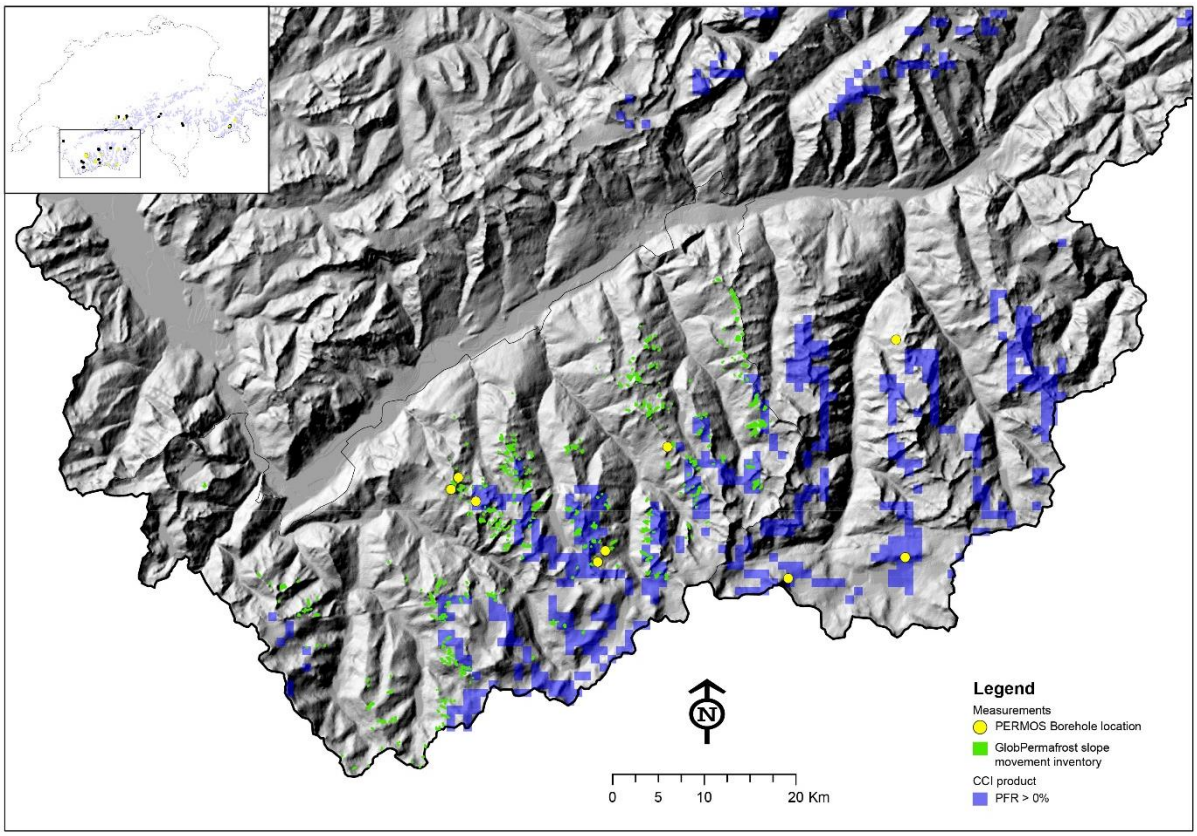

Figure 5.4. Overview of the simulated Permafrost_cci PFR in 2019 in Bas-Valais (CH) compared to the ESA GlobPermafrost slope movement inventory and PERMOS permafrost monitoring borehole locations.

Furthermore, the vast majority of inventoried ESA GlobPermafrost slope movement products are located outside of the simulated Permafrost_cci permafrost extent area and only six amongst the 12 PERMOS permafrost borehole sites are located within the simulated Permafrost_cci PFR permafrost extent area (Table 5.1). Again, a clear warm bias in the simulated permafrost temperatures is observed in the Swiss Alps.

Table 5.1. Permafrost_cci PFR Permafrost FRaction (%) time series from 1997 to 2019 at the location of the PERMOS boreholes (Overview on GTN-P PERMOS boreholes in [RD-5], Table 4.4).

YEAR	ATT	COR	FLU	GEN	LAP	MAT	MPB	MUR	RIT	SCH	STO	TSA
1997	-	14	14	29	-	43	29	29	-	-	86	-
1998	-	14	14	29	-	43	29	29	-	-	86	-
1999	-	14	14	14	-	43	29	29	-	-	86	-
2000	-	14	14	14	-	43	29	29	-	-	86	-
2001	-	14	14	14	-	29	29	14	-	-	86	-
2002	-	14	14	14	-	29	29	14	-	-	86	-
2003	-	14	14	14	-	29	29	14	-	-	86	-
2004	-	14	14	14	-	29	29	14	-	-	86	-
2005	-	14	14	14	-	29	14	14	-	-	86	-
2006	-	14	14	14	-	29	14	14	-	-	86	-
2007	-	14	14	14	-	29	14	14	-	-	86	-
2008	-	14	14	29	-	43	14	14	-	-	86	-
2009	-	14	14	14	-	43	14	14	-	-	86	-
2010	-	14	14	14	-	43	14	14	-	-	86	-
2011	-	14	14	14	-	29	14	14	-	-	86	-
2012	-	14	14	14	-	29	14	14	-	-	86	-
2013	-	14	-	14	-	29	14	14	-	-	86	-
2014	-	14	-	14	-	29	14	14	-	-	86	-
2015	-	14	-	14	-	29	14	14	-	-	86	-
2016	-	14	-	14	-	29	14	14	-	-	86	-
2017	-	14	-	14	-	29	14	14	-	-	86	-
2018	-	14	-	14		29	14	14	-	-	86	-
2019	-	14		14	-	29	14	14	-	-	86	-

6 SUMMARY

The growing demand for mapped permafrost products needs to accommodate user requirements that span permafrost regions from Scandinavia, Mongolia, China to higher latitude permafrost in North America, Greenland, Siberia and all altitude ranges from lowland to mountain permafrost. This results in high difficulties of assessing how the products perform in all regions across a wide range of latitudes, altitudes, climate zones, land cover, and lithologies. Permafrost_cci products were evaluated using pixel-based match-up analyses and expert knowledge. The validation and evaluation efforts also innovatively applied the Freeze-Thaw to Temperature (FT2T) product, an EO microwave-derived ground temperature, for comparison with the Permafrost_cci permafrost temperature product. PERMOS in Switzerland is specifically assessing the Permafrost_cci permafrost temperature and permafrost extent products for high-mountain permafrost regions, using in situ observations of surface temperature and borehole temperatures and the ESA GlobPermafrost rock glacier inventory on rockglaciers.

Permafrost_cci CRDPv2 provides 1 km pixel resolution ECV products on mean annual ground temperature (MAGT) at discrete ground depths (product name GTD), Active Layer Thickness (product name ALT) and Permafrost Fraction (product name PFR). All products cover the Northern hemisphere north of 30 °N in Arctic stereographic circumpolar projection. Permafrost_cci GTD, ALT and PFR time series from 1997 to 2019 come with an annual resolution. The match-ups were executed using a pixel-based approach. Permafrost_cci GTD is provided in 0.0, 1.0, 2.0, 5.0, and 10.0 m depth and depth-interpolated to fit the depths of the extensive in situ data set. The final match-up data set consists of temperature-depth time series in 0.0, 0.2, 0.25, 0.4, 0.5, 0.6, 0.75, 0.8, 1.0, 1.2, 1.6, 2.0, 2.4, 2.5, 3, 3.2, 4.0, 5.0, 10.0 and 20.0 m depth. The match-up data is standardized but still contains a large variability of match-up pairs in time, region, and, for example, MAGT reference depths.

Permafrost_cci GTD match-up evaluation between simulated Permafrost_cci and in situ measurements showed the following performance characteristics: Overall, the simulation dataset had a median MAGT bias of -1.12 °C (95% CI: -4.19 to 2.51 °C). Match-up pairs from in situ measurements with MAGT < 1°C and thus from reliable permafrost sites showed a much better performance with a median bias of 0.2°C, 95% CI: -4.09 to 3.18 °C, compared to the full dataset including in situ MAGT >= 1°C up to 5 °C MAGT along the southern boundary of the discontinuous and sporadic permafrost zone. Extreme residuals showed no obvious spatial clusters. However, a relatively large proportion of residuals >95% quantile were located across Alaska, specifically in the boreal regions. Residuals across depths were rather stable with slightly larger negative median biases in lower depths (0 to 3 m), mainly caused by negative biases in match-up pairs of warmer sites (MAGT >= 1°C) that are more abundant for the shallower depths.

As a consequence of the cold bias in the warm temperature range, the binary match-up of ’permafrost’ versus ‘no permafrost’ for Permafrost_cci PFR versus in situ MAGT ranges shows that PFR in the grid cell is overestimated compared to in situ-derived ‘no permafrost’ and MAGT ≤0.5 °C. Permafrost_cci PFR in the grid cell >0% occurs together with a wide range of ‘warm’ in situ MAGT >0 °C. Overall, the majority of match-up pairs (69.9%) were in agreement between the in-situ proxy and the Permafrost_cci simulation. Notably, the 100% and the 0% PFR had high percentage of agreement, with 97.04% and 91.03% match respectively. Geographically, most mismatches were located in the Eurasian southern boundary of the permafrost extent. The high agreement in the 100% and 0% Permafrost_cci

PFR groups was stable across years. In general, the agreement in the <100% and >0% groups increased towards the end of the time series (2019).

PERMOS investigations in the Swiss Alps showed in contrast a warm model bias of Permafrost_cci MAGT. The model bias ranges from +1.22°C at the surface to +1.81°C at 10 m depth. The extent of permafrost simulated by Permafrost_cci PFR is too restrictive. In the Swiss Alps, the lower limit of permafrost is usually found around 2600 m a.s.l. ±200 m whereas for Permafrost_cci PFR the lower limit is found around 3000 m a.s.l.. Furthermore, the vast majority of inventoried ESA GlobPermafrost slope movement products are located outside of the simulated Permafrost_cci permafrost extent area and only six amongst the 12 PERMOS permafrost borehole sites are located within the simulated Permafrost_cci PFR permafrost extent area. Permafrost_cci GTD in the Alps is systematically too warm at all depth and locations compared to in situ PERMOS MAGT. Permafrost_cci GTD values fit better the in situ observations near the surface and the warm model bias increases with depth at all sites. Although the absolute values are significantly different, both, the measured and the simulated MAGT, show a warming trend over the period 1997-2018. At depth, measured in situ MAGT in 2017 shows a more or less marked cooling effect. This is due to the extremely snow-poor winter 2016/17 in the Swiss Alps, which enabled the cold winter air temperature to cool the ground more efficiently. This effect is not reproduced in Permafrost_cci simulations, illustrating the difficulty to include snow effects in global models.

Ground temperatures based on satellite-derived freeze/thaw agree (FT2T) at selected cold sites for the overlap period 2008-2018. Deviations occur in the permafrost transition zone. In the presented cases, only one product (either CRDP or FT2T) agrees with in situ measurements. A bias of about 1.5°C can be observed for Alaska as well as Greenland.

For the Permafrost_cci ALT match-up analyses, we restricted the analysis on high-latitude to mid-latitude permafrost regions related to the Permafrost_cci model parameterization, excluding all sites in Mongolia, Central Asia, on the Tibetan Plateau (China) due to their different snow and subground regimes. Permafrost_cci ALT performance for in situ ALT with match-up pairs from China and Mongolia excluded is characterised by a median bias of 3 cm (95% CI: -11 to 123 cm). Differences in trends over time between Permafrost_cci and in-situ measurements are larger compared to the MAGT product (note ALT match-up sample size is also considerably smaller). The majority (58%) of Permafrost_cci ALT trends over time match the in-situ trends. Large residuals >1 m are obvious in the warmer permafrost zones in forested regions of Alaska, Canada and Central Siberia (Permafrost_cci negative bias with simulated shallow ALT versus deep in-situ ALT). Also, residuals >1.5 m cluster in Svalbard (Permafrost_cci positive bias with simulated deep ALT versus shallow in-situ ALT).

In summary, the Permafrost_cci permafrost temperature group (that we defined as GTD < 1°C) shows good performance with a median bias of 0.2°C for all depth layers and is well usable by the climate research community. Users of Permafrost_cci GTD products should however consider for their applications that Permafrost_cci MAGT in discontinuous, sporadic and non permafrost zones is characterized by a cold median MAGT bias of -1.47 °C. This leads in turn to too shallow simulated Permafost_cci active layer thickness in the permafrost continuous zones around the lower 60° Latitudes and to an overestimated areal extent of permafrost (Permafrost_cci PFR) in discontinuous, sporadic and extending to non-permafrost regions.

7 REFERENCES

7.1 Bibliography

Allard, M., Sarrazin, D. and L'Hérault, E. (2016): Borehole and near-surface ground temperatures in northeastern Canada, v. 1.4 (1988-2016). Nordicana D8, https://doi.org/10.5885/45291SL-34F28A9491014AFD.

Bartsch, A., Pointner, G., Leibman, MO, Dvornikov, Y., Khomutov, AV, Trofaier and AM (2017): Circumpolar ground-fast lake ice fraction by lake from ENVISAT ASAR late winter 2008, links to Shapefiles. PANGAEA, https://doi.org/10.1594/PANGAEA.873674, Supplement to: Bartsch, A et al. (2017): Circumpolar Mapping of Ground-Fast Lake Ice. Frontiers in Earth Science, 5(12), 16 pp, https://doi.org/10.3389/feart.2017.00012

Bergstedt, H. and Bartsch, A. (2020): Near surface ground temperature, soil moisture and snow depth measurements in the Kaldoaivi Wilderness Area, for 2016-2018. PANGAEA, https://doi.org/10.1594/PANGAEA.912482

Bergstedt, H., Bartsch, A., Duguay, C and Jones, B. (2020a). Influence of surface water on coarse resolution C-band backscatter: Implications for freeze/thaw retrieval from scatterometer data. Remote Sensing of Environment, 247, https://doi.org/10.1016/j.rse.2020.111911.

Bergstedt, H., Bartsch, A., Neureiter, A., Hofler, A., Widhalm, B., Pepin, N., and Hjort, J. (2020b). Deriving a frozen area fraction from Metop ASCAT backscatter based on Sentinel-1. IEEE Transactions On Geoscience And Remote Sensing, vol. 58, no. 9, pp. 6008-6019. https://doi.org/10.1109/tgrs.2020.2967364

Biskaborn, B. K., Smith, S. L., Noetzli, J., Matthes, H., Vieira, G., Streletskiy, D. A., Schoeneich, P., Romanovsky, V. E., Lewkowicz, A. G., Abramov, A., Allard, M., Boike, J., Cable, W. L., Christiansen, H. H., Delaloye, R., Diekmann, B., Drozdov, D., Etzelmüller, B., Grosse, G., Guglielmin, M., Ingeman-Nielsen, T., Isaksen, K., Ishikawa, M., Johansson, M., Johannsson, H., Joo, A., Kaverin, D., Kholodov, A., Konstantinov, P., Kröger, T., Lambiel, C., Lanckman, J.-P., Luo, D., Malkova, G., Meiklejohn, I., Moskalenko, N., Oliva, M., Phillips, M., Ramos, M., Sannel, A. B. K., Sergeev, D., Seybold, C., Skryabin, P., Vasiliev, A., Wu, Q., Yoshikawa, K., Zheleznyak, M., and Lantuit, H. (2019): Permafrost is warming at a global scale. Nature Communications, 10, 264. https://doi.org/10.1038/s41467-018-08240-4

Biskaborn, B. K., Lanckman, J.-P., Lantuit, H., Elger, K., Streletskiy, D. A., Cable, W. L., and Romanovsky, V. E. (2015): The new database of the Global Terrestrial Network for Permafrost (GTN-P), Earth Syst. Sci. Data, 7, 245–259.

Boike, J., Nitzbon, J., Anders, K., Grigoriev, M. N., Bolshiyanov, D. Y., Langer, M., Lange, S., Bornemann, N., Morgenstern, A., Schreiber, P., Wille, C., Chadburn, S., Gouttevin, I., and Kutzbach, L. (2018): Soil data at station Samoylov (2002-2018, level 1, version 1), link to archive. PANGAEA, https://doi.org/10.1594/PANGAEA.891140

Brown, J., Ferrians Jr., O.J., Heginbottom, J.A., Melnikov, E.S. (1997). Circum-Arctic Map. of Permafrost and Ground-Ice Conditions. US Geological Survey Reston.

Bryant, R.N., Robinson, J.E., Taylor, M.D., Harper, William, DeMasi, Amy, Kyker-Snowman, Emily, Veremeeva, Alexandra, Schirrmeister, Lutz, Harden, Jennifer and Grosse, Guido, 2017, Digital Database and Maps of Quaternary Deposits in East and Central Siberia: U.S. Geological Survey data release, https://doi.org/10.5066/F7VT1Q89.

Center for Northern Studies in Canada, CEN (2013): Environmental data from Northern Ellesmere Island in Nunavut, Canada, v. 1.0 (2002-2012). Nordicana D1, https://doi.org/10.5885/44985SL-8F203FD3ACCD4138.

GTN-P (2018): GTN-P global mean annual ground temperature data for permafrost near the depth of zero annual amplitude (2007-2016). PANGAEA, https://doi.org/10.1594/PANGAEA.884711

Kroisleitner, C., Bartsch, A., and Bergstedt, H. (2018): Circumpolar patterns of potential mean annual ground temperature based on surface state obtained from microwave satellite data, The Cryosphere, 12, 2349-2370, https://doi.org/10.5194/tc-12-2349-2018.

Naeimi, Vahid, Bartalis, Zoltan, Hasenauer, Stefan, and Wagner, Wolfgang (2009): An improved soil moisture retrieval algorithm for ERS and METOP scatterometer observations. IEEE Transactions on Geoscience and Remote Sensing, 47(7), 1999-2013, https://doi.org/10.1109/TGRS.2008.2011617

Paulik, Christoph, Melzer, Thomas, Hahn, Sebastian, Bartsch, Annett, Heim, Birgit, Elger, Kirsten and Wagner, Wolfgang (2014): Circumpolar surface soil moisture and freeze/thaw surface status remote sensing products (version 4) with links to geotiff images and NetCDF files (2007-01 to 2013-12). Department of Geodesy and Geoinformatics, TU Vienna, PANGAEA, https://doi.org/10.1594/PANGAEA.832153

Wang, K. (2018): A synthesis dataset of near-surface permafrost conditions for Alaska, 1997-2016. Arctic Data Center, https://doi.org/10.18739/A2KG55.

7.2 Acronyms

ALT	Active Layer Thickness
AWI	Alfred Wegener Institute Helmholtz Centre for Polar and Marine Research
B.GEOS	b.geos GmbH
CALM	Circumpolar Active Layer Monitoring
CC3	Permafrost_cci CryoGrid 3
CEN	Center for Northern Studies in Canada
CCI	Climate Change Initiative
CRDP	Climate Research Data Package
ECV	Essential Climate Variable
EO	Earth Observation
ESA	European Space Agency
FT2T	Freeze-Thaw to Temperature
GAMMA	Gamma Remote Sensing AG
GCOS	Global Climate Observing System
GCW	Global Cryosphere Watch
GT	Ground Temperature
GTD	Ground Temperature per Depth
GTN-P	Global Terrestrial Network for Permafrost
GTOS	Global Terrestrial Observing System
GUIO	Department of Geosciences University of Oslo
IASC	International Arctic Science Committee
IPA	International Permafrost Association
IPCC	Intergovernmental Panel on Climate Change
MAGT	Mean Annual Ground Temperature
NSIDC	National Snow and Ice Data Center
PE	Permafrost Extent
PERMOS	Swiss Permafrost Monitoring Network
PFR	Permafrost FRaction
RD	Reference Document
TSP	Thermal State of Permafrost
UNIFR	Department of Geosciences University of Fribourg
URD	Users Requirement Document
WMO	World Meteorological Organisation